ADSORPTIVE REMOVAL OF ARSENIC FROM WATER BY CHEMICALLY MODIFIED RICE HUSK

A DISSERTATION SUBMITTED FOR THE PARTIAL FULFILLMENT OF THE REQUIREMENTS FOR THE MASTER OF SCIENCE DEGREE IN CHEMISTRY

Submitted by

MENUKA RANA

Symbol No. 1445/075

T. U. Regd. No: 5-2-48-324-2014

CENTRAL DERPARTMENT OF CHEMISTRY

INSTITUTE OF SCIENCE AND TECHNOLOGY

TRIBHUVAN UNIVERSITY

KIRTIPUR, KATHMANDU, NEPAL

April, 2024

CERTIFICATE OF APPROVAL

This dissertation work entitled "**Adsorptive Removal of Arsenic from Water by Chemically Modified Rice Husk**" by Menuka Rana under the supervision of Professor. Dr. Megh Raj Pokhrel, Central Department of Chemistry, Tribhuvan University, Nepal and co-supervision of Asst. prof. Dr. Bhoj Raj Poudel, Tri-Chandra Multiple Campus, Kathmandu, Nepal is hereby submitted for the partial fulfillment of a Master's Degree of Science (M. Sc.) in Chemistry. This dissertation has not been submitted to any other University or institution previously for the award of a degree.

Supervisor

Prof. Dr. Megh Raj Pokhrel

Central Department of Chemistry

Tribhuvan University

Co-supervisor

Asst. Prof. Dr. Bhoj Raj Poudel

Tri-Chandra Multiple Campus

Tribhuvan University

External Examiner

Asst. Prof. Dr. Dasu Ram Poudel

Department of Chemistry

Tri-Chandra Multiple Campus

Internal Examiner

Asst. Prof. Dr. Bhanu Bhakta Neupane

Central Department of Chemistry

Tribhuvan University

Head of Department

Prof. Dr. Jagadeesh Bhattarai

Central Departrment of Chemistry

Tribhuvan University,

Kathmandu, Nepal

Date:……

RECOMMENDATION LETTER

This is to certify that this dissertation work "**Removal of Arsenic from Water by Chemically Modified Rice Husk**" has been conducted by **Menuka Rana** as a partial fulfillment for the requirement of an M. Sc. Degree in Chemistry under our supervision. This work has not been submitted for the award of any degree.

Supervisor

Prof. Dr. Megh Raj Pokhrel

Central Department of Chemistry

Tribhuvan University

Kathmandu, Nepal

Co-supervisor

Asst. Prof. Dr. Bhoj Raj Poudel

Tri-Chandra Multiple Campus

Tribhuvan University

Kathmandu, Nepal

DECLARATION

I, "Menuka Rana", hereby declare that the work presented here is genuine work done originally by me and has not been published or submitted elsewhere for any other degree. Any literature, data, or work done by others and cited in this dissertation has been given due acknowledgement and listed in the reference section.

Menuka Rana

Exam Roll No.: 1445/075

T.U. Regd. No.: 5-2-48-324-2014

Central Department of Chemistry

Tribhuvan University

Kathmandu, Nepal

ACKNOWLEDEMENTS

Completing this dissertation work is very desirable, and I would like to take this chance to thank everyone who has supported me in this journey. I would like to convey my appreciation to the esteemed supervisor of this research, Prof. Dr. Megh Raj Pokhrel of the CDC, TU, for all his help, continuous support, motivation, guidance, and invaluable feedback. I would like to acknowledge the UGC, Nepal for providing me a grant to take-out this dissertation. I am grateful to the respected co-supervisor, Asst. Prof. Dr. Bhoj Raj Poudel, for all his assistance and advice throughout the project.

I prompt my profound appreciativeness to Prof. Dr. Jagadeesh Bhattarai, Head of the CDC, for giving me the necessary physical conveniences to conduct this study. I am also obliged to all the respected Professors and all the staff of CDC. I am obliged to CDC for recording FTIR spectra. I am extremely grateful to Dr. Kisan Chhetri, JBNU, Korea for recording SEM, XRD, EDS and elemental mapping. I greatly appreciate my seniors, Krishna Subedi, Sabin Dhungana and Sunil Bhandari for their feedback, and excellent encouragement. I am thankful to my friend Anisha Banjara and Anup Adhikari. Lastly, I am extremely grateful to my family members for their unwavering support and ongoing encouragement during the process.

Menuka Rana

LIST OF ABBREVIATIONS AND SYMBOLS

mg/L	Miligram per litre
μg/L	Microgram per litre
C_i	Initial concentration
C_e	Equilibrium concentration
qe	Amount adsorbed at equilibrium
qm	Maximum amount adsorbed
qt	Amount adsorbed at time 't'
λmax	Maximum wavelength
nm	nanometer
RH	Rice Husk
Zr(IV)-RH	Zirconium(IV) loaded Rice Husk
% A	Percentage Adsorption
% R	Percentage Removal
ppm	Parts per million
rpm	Revolutions per minute

ABSTRACT

Arsenic is gaining attention worldwide due to its widespread occurrence in natural environments, particularly in groundwater, and its significant health risks to human populations. Research is ongoing to optimize bio-sorbent materials and develop efficient technologies for arsenic removal. In this work, As(III) has been extracted from aqueous solution using rice husk, a significant agricultural waste loaded with Zr(IV), or Zr(IV)-RH. The adsorbent was characterized using FTIR, SEM, XRD, and EDX techniques. The results of the experiment indicate that Zr(IV)-RH has a good adsorption capacity (q_{max} = 38.45 mg/g at pH = 9). It's desorption rate can reach 92.21% with 2M NaOH, indicating that it is a promising regenerable adsorbent. At a rotational speed of 190 rpm, the effective contact time was 5 hours. In the course of studying adsorption kinetics, experimental data was fitted with PSO kinetic models and Langmuir isotherm models. The favorability of the adsorption process was validated by the value of R_L between 0 and 1.

Phosphate demonstrated the greatest inhibition to the adsorption of As(III) onto Zr(IV)-RH among the co-existing ions, sulfate, silicate, and nitrate. The pH_{pzc} value of Zr(IV)-RH was determined to be 10. As a result, the studied Zr(IV)-RH adsorbent may prove to be a useful, affordable, environmentally acceptable, and efficient material for the removal of arsenic from contaminated water.

Keywords: Rice husk, As(III), adsorption isotherm, kinetic model, co-existing ions.

सोधसार

यो अध्ययन आर्सनिक(III) हटाउने जलीय समाधानबाट जिर्कोनियमयुक्त धानको भुसलाई [Zr(IV)-RH] जैविक सेाखानाकाे रूपमा प्रयोग गरेर ब्याच प्रयोगहरूमा अनुसन्धान गरियो। पी. एच, सम्पर्क समय, सोखने खुराक आर्सनिक (III) एकाग्रता र सह. अवस्थित आयनहरूको प्रभाव जस्ता सेाखानाहरूलाई असर गर्ने विभिन्न पारामिटरहरू पनि जाँच गरियो। सो एडसेारबेट विशेषता FTIR, XRD र SEM-EDX विश्लेषणद्वारा गरिएको थियो। परिमाणले पत्ता लगायो कि ९ पी. एचमा अधिकतम सेाखाना ८५% को हटाउने प्रतिशतको साथ अवलोकन गरिएको थियो। ३०० मिनेटको सम्पर्क समयमा अधिकतम सेाखानामा नोट गरियो। [Zr(IV)-RH] मा आर्सनिक(III) को रूपमा अधिकतम सोखना क्षमता ३८.४५ मिलीग्राम प्रति ग्राम थियो। प्रयोगात्मक डाटा Langmuir Isotherm र Pseudo second-order मोडलमा राम्रोसँग फिट गरियो। आर्सनिक(III) को रूपमा ट्रेस एकाग्रता जुन जलीय समाधानमा अवस्थित छ(१ मिलिग्राम प्रतिग्राम) पर्याप्त रूपमा विश्व स्वास्थ्य संगठन मनक (१० मिलिग्राम प्रतिग्राम) ५ ग्राम प्रतिलिटर प्रयोग गरेर अनुसन्धान गर्न सकिन्छ। सह- अवस्थित आयनहरू जस्तै नाइट्रेट, सिलिकेट र सल्फेटले सेाखना आर्सनिक थोरै प्रभाव पर्यो जबकि फोस्फेट उपस्थित हुँदा सबैभन्दा कम सेाखना अवलोकन गरियो। NaOH को फरक एकग्रता (0.01M देखि 2M) प्रयोग गरी अवशोषण प्रतिशतको खोज गरियो, जसमा NaOH एक प्रभावकारी eluent साबित भयो जसले ९२.२१% भन्दा बढी प्रतिशत अवशोषण गरिएको पाइयो। त्यसकारण अनुसन्धान गरिएको [Zr(IV)-RH] एडसेारबेट एक आशाजनक, कम लागत, वातावरण मैत्री र आर्सनिक प्रदूषित पानीको विघटनको लागि प्रभावकारी सामग्री हुन सक्छ।

शब्द कुञ्जीहरू: आर्सनिक(III), जैविक सेाखाना, जिर्कोनियमयुक्त धानको भुस [Zr(IV)-RH], सेाखना Isotherm र kinetics , सह अवस्थितआयन

TABLE OF CONTENTS

LIST OF FIGURES

LIST OF TABLES

CHAPTER I

INTRODUCTION

1.1 General Introduction

“Arsenikon” is a Greek word that means “bold” or “potent”. Arsenic has also been utilized as a medicine from ancient times, even though it may seem strange given its reputation as being deadly. It was employed as a green pigment in wallpaper, paint, linens, and other typical household things in the 19th century. In addition, arsenic finds extensive use in a variety of other industrial sectors, including insecticides and preservatives. Arsenic has been employed both as a blessing and a curse, whether as a toxin, a medication, a pesticide, a preservative or for any other reason. Depending on how it is used it may be beneficial or harmful (Parascandola, 2012).

Arsenic comes in two forms: inorganic and organic. The most hazardous kind is thought to be inorganic (Velazquez-Jimenez et al., 2018). Inorganic As can be presentas -3,0,+3,+5 oxidation states with arsenates (+5) in oxidizing environments and arsenites (+3) in mildly reducing conditions (Lee, K.S. et al., 2015).

Pentavalent species are;

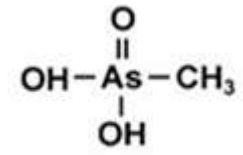

Monomethylarsonic Acid

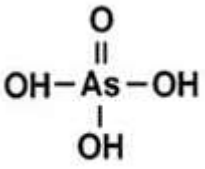

Arsenic Acid, Arsenate

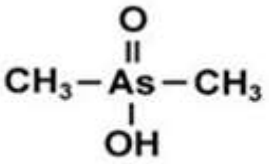

Dimethylarsinic Acid

Trivalent species are;

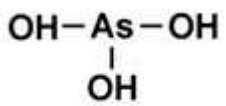

Arsenious Acid, Arsenite

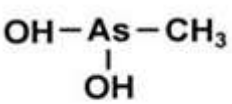

Monomethylarsonous Acid

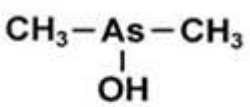

Dimethylarsinous Acid

Arsenic is not frequently found in nature as an element but is more frequently found as the iron-sulfur complex arsenopyrite (FeAsS) or the sulfide compounds orpiment

(As_2O_3) and realgar (As_4S_4) (Parascandola, 2012). Additionally found in rocks like metamorphic, igneous and sedimentary; in soil, air, water and living beings (Tamaki &Frankenberger, 1992). It is often associated with metal ore deposits, serving as a "Pathfinder element" for miners. Heat can induce As to sublimate into a gas with a distinct garlic, smell, despite the fact that the majority of As compounds have neither taste or smell. When rocks were hammered by hammers a strong odor produced that allowed miners to identify As in rock was released. Environmental problems with As began with leaching from mining tailings in the US, the UK, Australia, Thailand, Mexico, Canada. As-polluted aquifers in Ghana, Bangladesh, Argentina, Ghana, Nepal and Vietnam resulted in chronic As-poisoning. Among them Bangladesh has the worst condition. It is found in water, soil, plants, air and all other living organisms and its existence in food is not surprising (Jones, 2007).

Groundwater is primarily contaminated by As from natural processes like weathering minerals, anthropogenic sources like poorly managed discharge from industries and As containing pesticides (Shakoor et al., 2019). Arsenic is very toxic in nature. Its negative effects are primarily induced by inactive enzymes in the cellular energy system, where As combines with (-SH) groups of proteins and enzymes, limiting their catalytic function (Vahidniaet al., 2007). In oxidizing environment arsenic sulfide converts into arsenic trioxide (Mandal& Suzuki, 2002).Arsenic oxide dissolves easily in water and it has no taste, smell or color. Hence it is challenging for the victim to realize that they are being poisoned. Since it is a cumulative poison, small doses taken over an extended length of time can lead to death (Parascandola, 2012).

Arsenic toxicity will be determined by physical characteristics such as form (gas, solution or powder) and particle size. In addition chemical parameters (valence, solubility and the presence of other impurities), exercise level, gender ,age, health status and the route of exposure also affect it's toxicity (Jones, 2007). Arsenic toxicity can be acute or chronic. Acute toxicity is resulting from short –term exposure to high arsenic levels whereas chronic toxicity is caused by long-term exposure to low arsenic levels (Mandal & Suzuki, 2002). Symptoms of acute arsenic poisoning, like vomiting, pain in abdomen, nausea, diarrhea, were often easily confused with those of other common illnesses (Hughes et al., 2011). Chronic poisoning can result in keratosis, hyperkeratosis, cancer, heart problems, nerve damage, miscarriages, preterm birth etc. Thus, the WHO have set maximum acceptable limit of 10ppb for arsenic (Velazquez-

Jimenez et al., 2018). Nearly 50% of Nepal's population are in Terai region and majority of them gets their drinking water from groundwater sources. However most of these sources are contaminated with bacteria and As. Several Terai districts in Nepal have been primarily affected by arsenic poisoning (Timalsina et al., 2021).

The threat of arsenic contamination of drinking water resources seems worldwide. Thus, it is urgently needed to remove arsenic from drinking water. Numerous approaches have been employed to remediate As from water as shown in the following diagram (Rahidul Hassan, 2023).

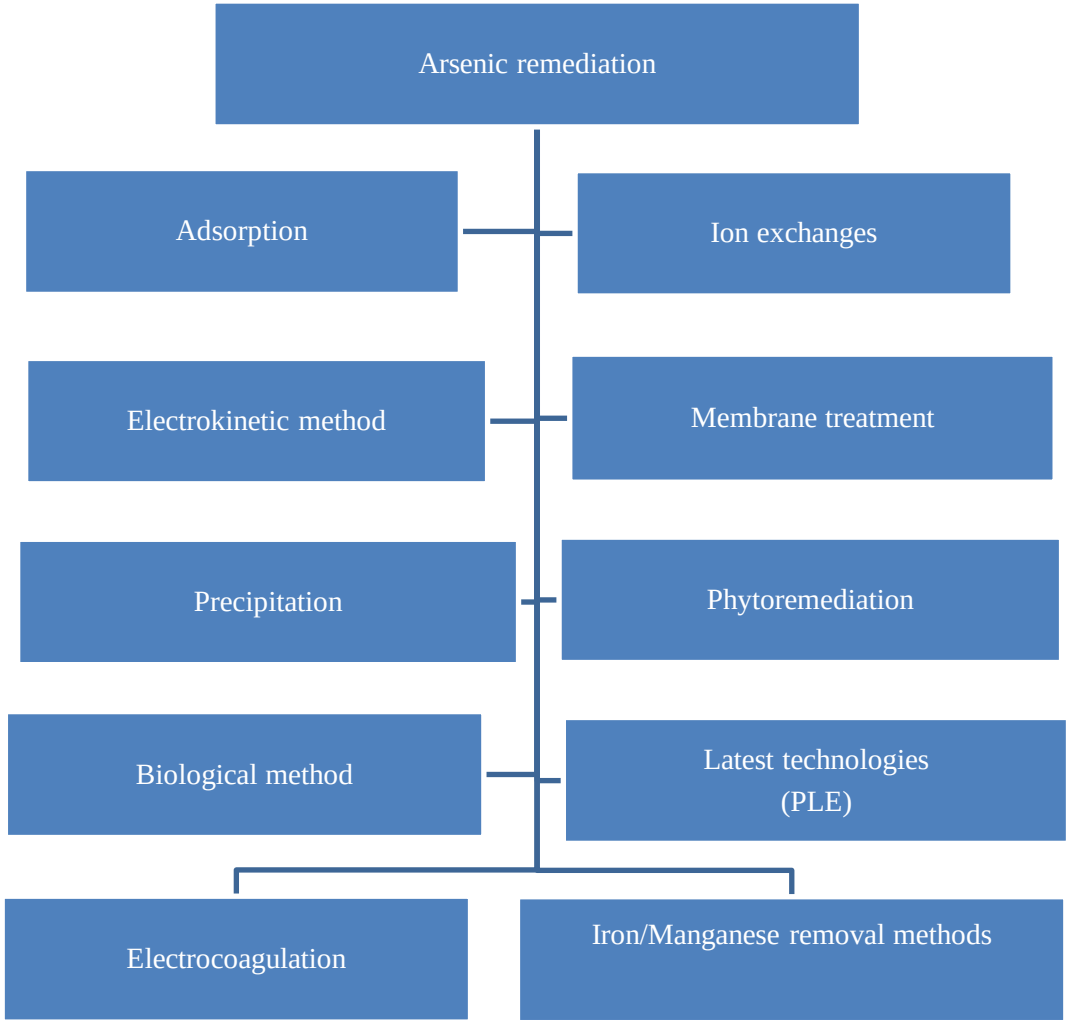

Figure 1: Techniques of Arsenic removal

In terms of ease of use and cost of operation, adsorption process have been proven to be more effective than other approaches indicated above (Velazquez-Jimenez et al., 2018).Chemically modified biosorbents had greater adsorption capabilities than raw or unmodified biosorbent (Al-Rashdi et al., 2011).

1.2 Rice Husk Loaded with Zirconium (IV) as Potential Adsorbent

The elimination of metal ions has been examined using a range of agricultural waste products, including wheat, bran, husk, bark, coconut shells, coffee beans, sugar cane baggage, apple banana and orange peels, maize corn cobs, tea waste sunflower stalks etc. However very little research has been done on using raw rice husk to remove arsenic from groundwater (Asif & Chen, 2017a). In the present study chemically altered Zr-loaded rice husk was employed for removing arsenite from water.

Rice husk is composed of 15–25% silica, 28–30% cellulose, 25–30% lignin, and 10-15% hemi-cellulose. Given its high silica content, it appears to be able to offer adequate structural strength without requiring cross-linking (Shrestha et al., 2021). It contains various functional groups (Montalvo-Andía et al., 2022). These functional groups help in metal complexation and remove metal ions (Shakoor et al., 2019).

Table 1: Properties of rice husk (Shukla, 2020)

S.N.	Properties	Values
1	Bulk density	86-114kg/m^3
2	Moisture contents	8.68-10.44%
3	Particle size	0.212-0.850 mm
4	Calorific values	3000K Cal/kg

This research suggests the usage of tetravalent zirconium ion for arsenic removal from aqueous solutions. Zirconium is the fourth transition metal. Earth's crust contains 0.016% of it. Zr oxides are chemically stable, non-toxic, and stable to acids /base. Zirconium in its hydrated form can produce abundant OH^- ions and H_2O molecule (Biswas et al., 2008a; Zou et al., 2020).

Silica, a protective layer on rice husks may cause insufficient adhesion between functional groups and various adsorptive ions. Adhesion capacity can be enhanced by removing silica and surface impurities. For this chemical treatment is required. Studies have demonstrated that alkali removes lipids, waxes, lignin, exposes reactive functional groups and increases fiber roughness (Chowdhury et al., 2011). In the present study calcium hydroxide [$Ca(OH)_2$] is selected for chemical treatment of rice husk.

1.3 Adsorption Study

Adsorption is the term used to describe the gathering of a specific component at the interface or surface between two phases, typically with a higher density compared to the bulk. An adsorbate is a substance that is attaches to a solid surface and adsorbent is the surface of the solid to which it is attached. When contaminated water is shaken with a finely divided solid, the contaminants stick to the solid surface and equilibrium is created. At this point the concentration of contaminants adsorbed and, in the water, become constant. The adsorption isotherm expresses how the equilibrium quantity of adsorbed pollutants in water changes with temperature. Adsorption isotherm can be explained using models like Langmuir, Freundlich and other parameters (Ali & Gupta, 2006).

A molecule can attach to surfaces through physical or chemical adsorption. Weak Vander Waal's force forms between the adsorbate and the adsorbent during physical adsorption whereas in chemical adsorption strong covalent bond occurs between adsorbate and adsorbent (Atkins & Paula, 2014). In this investigation Batch adsorption test has been done to study the adsorption behavior of the material.

1.4 Batch Experiment method

A stock solution of arsenic will be prepared in distilled water. 250ml flask will be used with required amounts of adsorbent and arsenic solution. The flask will be shaken for 24 hours at controlled pH and temperature to assure complete equilibrium. Shaking afterwards, the solution will undergo filtration and the level of arsenic will be evaluated spectrophotometrically by using molybdenum blue method. The batch experiment study will be executed by altering the parameters like contact time, initial metal ion or non-metallic ion concentration, temperature, pH etc. The percentage of arsenic removal will be calculated by using formula (Dhakal et al., 2005).

The percentage of arsenic removal will be calculated as:

$$R=\frac{C_o\text{-}C_e}{C_o}\times 100 \text{.....(i)}$$

where Co and C_e signify the initial and final concentration of adsorbate, respectively. For every concentration of adsorbate at equilibrium, the adsorbent's arsenic biosorption capacity, q (mg/g) will be calculated as follows.

$$q = \frac{C_o - C_e}{W} \times V \text{.....(ii)}$$

Where V stands for the volume of aqueous solution (L) and W is the weight (g) of dry biosorbent.

1.5 Instrumental Characterization

Bio adsorbent will be characterized by FTIR, XRD, EDX and SEM.

1.5.1 FTIR

Information about a molecule's structure and functionality can be obtained simply by studying the infrared spectrum. FTIR is the preferred infra-red spectroscopy method due to its non-destructive nature, speed, sensitivity, and precision compared to older techniques (Ismail et al., 1997; Qu et al., 2017).

1.5.2 XRD Analysis

It is utilized to examine phase, composition, texture, and many more in powder, solid or even liquid samples. After that, detection, processing, and counting of these diffracted X-rays takes place. The powdered material's random orientation should allow for the detection of all possible lattice diffraction directions by scanning the sample across a range of 2θ angles.

1.5.3 SEM

It is a suitable method for analyzing materials on a nanometer to micrometer scale, producing precise images at high magnifications (Mohammed & Abdullah, 2018). The SEM delivers surface morphology (Ural, 2021). SEM uses a low-energy electron beam to scan a material's surface, resulting in photon and electron emission. Signals are detected by using detectors for material characterization.

1.5.4 EDX Analysis

EDX is based on the incident beam electrons producing distinctive X-rays in the specimen's atoms. Elastic and inelastic scattering are two basic physical events that involve electron direction changes without energy loss and energy loss without direction change respectively. Elastic scattering and inelastic scattering determine the shape and size of interaction volumes. Atoms ionize and emit characteristic X-rays,

which are characteristic of the element. These X-rays can be measured by a photon-energy sensitive detector, providing information on the elements present in the specimen, and their energy depends on the element's atomic number (Scimeca et al., 2018).

1.6 Chemical Characterization

1.6.1 Determination of pH_{pzc}

At this pH of point zero charge, the positive and negative surface sites have equal charge. Sorbent surfaces are negatively charged at pH> pH_{pzc}, interacting with +vely charged adsorbate. While at pH< pH_{pzc} a biosorbent surface is +vely charged and attract-vely charged adsorbate (Fiol&Villaescusa, 2009). The PZC of organic substrates is frequently determined using the salt addition method. There are several names for the salt addition method, including the batch equilibration method, the powder addition method, and the solid addition method. Its simplicity and speed of execution are its merits (Bakatula et al., 2018). Since As(III) appears in aqueous solution in arsenite anion, it is possible that a positively charged surface will promote the most favorable adsorption process.

Both adsorption equilibrium and adsorption rate are essential elements in any adsorption process. These two points are discussed below;

1.6.2 Adsorption Isotherm

Isotherm model provides specific parameters for each system (Saadi et al., 2015). The well-known adsorption isotherms are Langmuir, Freundlich, Tempkinand Redlich-Peterson (Guo& Wang, 2019). Among them two isotherms are explained below.

Langmuir Adsorption Isotherm

It assumes a monolayer adsorption on the surface of adsorbate. Adsorption energy is uniform and adsorbent surface is homogeneous for all sites. No more adsorption may occur at a location after a pollutant has occupied it due to the intermolecular forces decrease quickly with increasing distance (Saadi et al., 2015).

$$q_e = \frac{q_o K_L C_e}{1 + K_L C_e} \quad \text{.....(iii)}$$

It can be changed into a linearized form as follows:

$$\frac{C_e}{q_e} = \frac{1}{K_L q_o} + \frac{C_e}{q_o} \text{.....(iv)}$$

where K_L is Langmuir equilibrium constant. At equilibrium q_e is adsorption capacity. The separation factor, also referred as the equilibrium parameter, or R_L, is a significant Langmuir model parameter that determines whether surfactant adsorption is favorable or unfavorable. In mathematical term, it can be represented as

$$R_L = \frac{1}{1+K_L C_o} \text{.....(v)}$$

Adsorption is generally considered advantageous when $R_L < 1$ and irreversible when $R_L \geq 0$, linear if $R_L = 1$, and unfavorable if $R_L > 1$ (Kalam et al., 2021).

Freundlich Adsorption Isotherm

Multilayer adsorption can be addressed using this model. According to this model, active sites and their energies are assumed to disperse exponentially on the diverse adsorbent surface (Saadi et al., 2015). The expression of it is given below:

$$q_e = bC_e^{\frac{1}{n}} \text{..... (vi)}$$

where adsorption intensity, or surface heterogeneity, is expressed as 1/n while b is the biosorption capacity stated in mg/L. Favorable biosorption happens when $0 < 1/n < 1$. When $1/n > 1$, unfavorable adsorption takes place and becomes irreversible at $1/n = 1$.The linear equation is expressed as (Kalam et al., 2021):

$$\text{`}\ln q_e = \ln b + \frac{1}{n}\ln C_e \text{.....(vii)}$$

1.6.3 Adsorption Kinetics

Adsorption rate information is provided by kinetic studies and is crucial for system design and practical implementation. Moreover, it contributes to the revelation of the adsorption mechanism (Nguyen et al., 2014). Many models have been formulated to explain the biosorption kinetics, including the pseudo first order (PFO) model, the pseudo second order (PSO) model (Wang &Guo, 2020).

PFO Kinetic Model

Largergren presented the PFO equation in 1898. Its differential form is as follows:

$$\frac{dq}{dt} = K_1(q_e - q) \ldots\ldots\ldots (viii)$$

where t = time (min), k_1 = rate constant (1/min), and q = adsorption capacity (mg/g). When t = 0 and integrating with the q=0, above equation gives,

$$q=q_e(1-\exp(-kt)) \ldots\ldots\ldots (ix)$$

The linearized form is,

$$\ln\left(\frac{q_e}{q_e-q}\right) = k_1 t \ldots\ldots\ldots (x)$$

PSO Kinetic Model

According to this model, the uptake rate for the available surface sites is second order.

$$\frac{dq}{dt} = K_2(q_e - q)^2 \ldots\ldots\ldots (xi)$$

where k_2 denotes PSO rate constant. The meanings of other symbols are identical to those found in the PFO model. The linearized form is obtained through rearrangement (Tan & Hameed, 2017).

$$\frac{t}{q} = \frac{1}{K_2 q_e^2} + \frac{t}{q_e} \ldots\ldots\ldots (xii)$$

1.6.4 Influence of Interfering ions

Anions like as sulfate, phosphate, nitrate, carbonate, silicate and other ions, may undergo competition with oxy-anion of arsenic for active sorption sites and hence lower the adsorbents' ability to remove arsenic. It has been shown that these coexisting anions lessen the interaction between the two anions and form inner-sphere complexes with arsenic. As the concentration of anions increases and the pH changes, the effects usually become more pronounced (John et al., 2018).

1.6.5 Desorption Studies

Adsorption exhausts adsorbents pores due to adsorbed material, necessitating desorption and regeneration for effective and economical removal. Few literatures

exist on desorption and regeneration, but understanding metal adsorption mechanisms can effectively achieve desorption. The proper eluent, regenerating chemical, and metal adsorption mechanism are necessary for desorption and regeneration process, which allows partial or total reversible regeneration of the used adsorbent.

Since arsenic is not much of use, recovery is not economical in this case, so recovery is not recommended. In order to minimize the demand for new adsorbent and the expense of disposing of exhausted adsorbent, adsorbent regeneration should be a low-cost procedure that aims to reuse the adsorbent for as many cycles as feasible.

1.7 Objectives of the Study

1.7.1 General Objectives

The objective of the study was to explore base treated modified rice husk loaded with Zr(IV) as an adsorbent for arsenic removal.

1.7.2 Specific Objectives

The specific objectives were given below.

a) To modify naturally occurring rice husk by alkali treatment followed by Zr (IV) loading.

b) To characterize adsorbent using SEM, XRD and FTIR spectroscopy.

c) To evaluate the q_{max} of Zr-loaded rice husk (Zr-RH).

d) To compare the RH and Zr-RH as adsorbents to remove arsenic.

e) To study the influence of interference ion like silicate, nitrate, phosphate and sulfate on adsorption.

f) To figure out the adsorption behavior of arsenic onto the adsorbent through batch adsorption test.

g) To compare the efficiency of bio-sorbents with commercially available adsorbents.

CHAPTER II

LITERATURE REVIEW AND RESEARCH GAPS

2.1 Review of Literature

The traditional method, which uses metal ions in co-precipitation-coagulation, has disadvantages including managing polluted sludge improperly and separating and filtering it. Eco-friendly wastewater treatment systems can be developed by utilizing biomass and natural products for arsenic adsorption. Adsorbents at minimal cost can be obtained in large quantities from biological materials, including alginate, methylated yeast biomass, fungal biomass, bio-char, and chicken feathers (Biswas, Inoue et al., 2008a).

Lee et al., (1999) studied the elimination of arsenate from aqueous solution using quaternized rice husk (QRH). The findings indicated that sorption was temperature- and pH-dependent, with q_{max} of 18.98 mg g^{-1} at 28±2°C and pH 7.5. Input concentration, flow rate, and bed depth all influenced breakthrough.

Amin et al., (2006) explored the application of rice husk to remove arsenic from aqueous solutions. Adsorption was performed without pretreatment. The result exhibited the q_{max} arsenite and arsenate at 100µg/L initial concentration and 6 g adsorbent dose.

Tian et al., (2011) utilized wheat straw with Fe_3O_4 to create magnetic bio-adsorbents. The wheat straw template with a higher Fe_3O_4 content increased adsorption capacity. The maximum As (III) biosorption occurred at pH 7–9. Regeneration was performed using a NaOH solution.

Soleimani et al., (2011) examined the adsorption of arsenic ions on a poly-aniline/rice husk (PAn/RH) nanocomposite. The optimal conditions to remove arsenic were pH 10, 10 g/L biosorbent dosage, and contact duration of 30 minutes. The q_{max} was 34.48 mg/g.

Kamsonlian et al., (2012) studied the adsorption of arsenite from water by mango leaves powder and rice husk. The optimal pH was found to be 7 and 6 for MLP and RH, respectively. The Freundlich isotherm model adequately explained equilibrium

data. The best eluent were sodium hydroxide, nitric acid, ethylene di-aminetetra acetic acid, and hydrochloric acid.

Pehlivan et al., (2013) showed a using of Fe-coated rice husks for removing As(V) from aquatic media. The pH exhibited a noteworthy impact on removing As(V) ions, with a maximum percentage of 94% at pH 4.0.

Zirconium polyacrylamide, a novel hybrid material, was introduced by Mandal et al., (2013) to eliminate arsenic (III) from synthetic water. The material showed a maximum removal efficiency of 98.22% and was stable up to 680°C. Second-order kinetics governed the adsorption process, and q_{max} were 0.20 and 0.80 mg/g.

Agrafioti et al., (2014) employed bio-char adsorbents derived from rice husk, sewage sludge to remove As (V), Cr (III), and Cr (VI) from water. Bio-char made from sewage sludge was most effective to remove 89% of hexavalent chromium and 53% of arsenate.

Chand et al., (2015) demonstrated arsenite and arsenate biosorption on iron-loaded sugarcane bagasse. The adsorption was an adsorbate-dependent process, with optimal adsorption capacities at pH 8 and pH 5 for arsenite and arsenate respectively. The optimal dosase were 200 mg and 100 mg, respectively.

Zhang et al., (2016) discovered Ce-CNB, a new ultrafine nano-biosorbent, which effectively removed arsenic from contaminated water. The nano-composite was treated with 5.8 liters of As(III)-contaminated water, achieving an effluent concentration below WHO standards. Study showed that arsenite and hydroxyl groups form mono-dentate and bi-dentate complexes, which are involved in the adsorption mechanisms.

Mondal & Garg, (2017) found that basic chemical or physical therapies cannot eliminate harmful heavy metals. Activated carbon was utilized in his research. The result exhibited the metal ions and acidic surface functional group of AC formed surface complexes.

Chaudhry et al., (2017) used zirconium oxide-coated sand for removing toxic As (III), from aquatic environment. The study found that the q_{max} was136.98 µg/g. The biosorption process fitted PSO kinetics and film diffusion steps controlled it.

Asif & Chen, (2017b) proposed that fixed bed column treatment system is a simple, easy-to-use domestic approach for arsenic removal in local areas. It effectively removed arsenic from 15-70 ppb concentrations. The system's practical applicability was tested under various conditions, and it has recycling potential for use in cement/insulation panels and roof sheets.

Pillai et al., (2020) used rice husk modified with Fe-oxide for removing arsenic. The biosorbent was synthesized by the co-precipitation technique. The result showed a removal percentage of 95% and q_{max} of 82 mg/g in 60 minutes. The biosorption process showed a 56% removal rate during regeneration as observed through Langmuir models and PSO.

Cuong et al., (2022) developed a high-performance method of removing arsenic from groundwater using an active biochar composite filter and electrosorption by capacitive deionization (CDI). The active BC technique demonstrated quick removal rates and high maximal arsenic removal capacities.

Javed et al., (2023) combined rice husk ash (RHA) and Fe-oxide NPs for removing arsenic from drinking water. It effectively eliminated 98% of the arsenic metal from a 40 ppm groundwater sample after being transformed into a purification cartridge. The rice husk treated with iron oxide has an adsorption capacity of 25.06 mg/g. After being reused, the stability of the absorbent was also investigated.

2.2 Research gap

There are various methods available, including ion exchange, reverse osmosis, membrane processes, precipitation, crystallization, etc., for the removal of higher concentrations of arsenic. However, the removal of trace concentrations of arsenic is challenging. In real practice, the above-mentioned methods are expensive for developing countries like Nepal. This study will develop a new, cheap, effective, eco-friendly, and promising material to remedy this research gap. The previous researches have explored the usage of biomass-based adsorbent to remove heavy metals, including arsenic from water. To the best of our knowledge, a novel method for removing arsenic from aqueous solutions will include chemically modifying rice husk (base-treated, followed by Zr(IV) loaded.

CHAPTER III

MATERIALS AND METHODS

3.1 Reagents

All the reagents utilized were of the analytical or laboratory grade, which are listed in Table 1. These Reagents were used without any further purification steps.

Table 2: Reagents used in research

S.N.	Name of the Chemicals	Manufacturer name	% Purity
1.	Arsenic Trioxide (As_2O_3)	S.D. fine chemicals	95%
2.	Ammonium heptamolybdate [$(NH_4)_4Mo_7O_{24}.4H_2O$]	Qualigens fine chemicals	98%
3.	Buffer Tablets (pH of 4, 7 and 9.2)	Qualigens fine chemicals	
4.	Calcium hydroxide $Ca(OH)_2$	Qualigens fine chemicals	95%
5.	Hydrochloric acid (HCl)	Qualigens fine chemicals	97%
6.	Hydrazinehydrate ($NH_2NH_2.H_2O$)	Qualigens fine chemicals	99%
7.	Potassium permanganate ($KMnO_4$)	Qualigens fine chemicals	99%
8.	Sodium Chloride (NaCl)	Thermo Fischer Scientific	99.50%
9.	Sodium Hydroxide (NaOH)	Qualigens fine chemicals	99%
10.	Sodium Sulfate (Na_2SO_4)	Thermo Fischer Scientific	99%
11.	Sulfuric acid (H_2SO_4)	Qualigens fine chemicals	98%
12.	Zirconium Oxychloride Octahydrate ($ZrOCl_2.8H_2O$)	Himedia	99%

3.2 Instruments

- Laboratory mill (Grinder),
- Sieve number 212 mesh,
- Weighing Balance (Pioneer Company, GT 210V, USA),
- Rotary Flask Shaker (Model no. BST/RS-436, India),
- Digital pH meter (Deluxe pH meter Model, India),
- Spectrophotometer (Model 2306, India),

3.3 Preparation of Reagents

3.3.1 Preparation of 1000 ppm As (III) Stock Solution

About 1.32 g of arsenic trioxide was weighed. Subsequently, it was dissolved in 5 mL of a 10M NaOH solution. After vigorous shaking, the final volume was increased to 1000 mL in volumetric flask (VF) using distilled water (DW).

3.3.2 Preparation of Working Solution

The stock solution was serially diluted with DW to prepare the working As(III) solutions.

3.3.3 Preparation of Ammonium Molybdate Reagents

3.3.4 Ammonium Molybdate Reagent (I)

12.5 g of ammonium molybdate powder were dissolved in 87.5 mL of DW in a 500 mL VF. In a separate beaker, 200 mL of DW was carefully mixed with 140 mL of a strong H_2SO_4 solution. After cooling, it was added to a 500 mL VF containing an ammonium heptamolybdate solution and diluted with DW up to the mark.

3.3.5 Ammonium Molybdate Reagent (II), 5% (w/v)

20.05 g of ammonium molybdate were dissolved in 250 mL of DW in a 50 mL VF. Subsequently, 198 mL of reagent (I) was added to the same flask and allowed to cool. To obtain a 5% (w/v) solution, the mixture was diluted up to the mark of a 500 mL VF.

3.3.6 Ammonium Molybdate Reagent, 0.5% (w/v)

0.5%(w/v) of a working solution was prepared in 100 mL VF by diluting 10 mL of ammonium molybdate reagent (II) with DW up to the mark.

3.3.7 Preparation of 0.5M Hydrazine Hydrate ($NH_2NH_2.H_2O$) Solution

2.5 mL of concentrated hydrazine hydrate was taken in a 100 mL VF. The volume was made up to the mark to prepare a 0.5M hydrazine solution.

3.3.8 Preparation of 1.5N Sulfuric Acid (H_2SO_4) Solution

A 1.5N sulfuric acid solution was prepared in a 250 mL VF. 10.41 mL of concentrated H_2SO_4 solution was added to DW, and the volume was made up to the required mark.

3.3.9 Preparation of 0.1N HCl Solution

A 0.1N HCl solution was prepared by diluting conc. HCl 4.5 mL of conc. HCl was added to water in a 500 mL VF, and the volume was made up to the required level.

3.3.10 Preparation of Zirconium Nitrate Solution

1 gram of zirconium nitrate was dissolved in 50 mL of 2N nitric acid. The mixture was further dissolved in distilled hot water, and the volume was marked up to 250 mL in a beaker. Zr(IV) solution was obtained by filtering the turbid solution under hot conditions.

3.3.11 Preparation of NaOH solution

20 grams of NaOH pellet were dissolved in 100 mL of DW to make a 5M NaOH solution. The NaOH solutions with concentrations of 0.01M, 0.05M, 0.1M, 0.5 M, and 1M were prepared by serial dilution of 5M NaOH solution.

3.3.12 Preparation of Buffer solution

The buffer solutions were made by dissolving the required buffer tablets in DW in three different 100 mL VFs. Then the resulting solution was diluted up to the mark.

3.3.13 Preparation of Saturated $Ca(OH)_2$ Solution

15 g of calcium hydroxide was dissolved in 500 mL of DW for 24 hours. The solution was left for a few hours to allow any remaining undissolved $Ca(OH)_2$ to settle down. Then a clear solution, known as the saturated calcium hydroxide solution, was separated.

3.3.14 Preparation of 0.1N Potassium Permanganate ($KMnO_4$) Solution

In a 100 mL VF, 0.32g of $KMnO_4$ crystals were dissolved with DW, brought to a boil for one hour, allowed to cool, and then filtered through glass wool.

3.4 Preparation of Adsorbent

3.4.1 Preparation of Raw Rice husk

The rice husk was collected from Banepa, was rinsed with water multiple times and left to air dry. The dried rice husk was grinded in grinder and then sieved through <212-micron mesh to obtain uniform size. The biomass was again cleaned with DW until a clear solution was obtained. After which, it was dried for 24 hours at 65°C in a hot air oven. The dry powder was stored in a clean plastic bottle for further use as raw adsorbent (raw rice husk-RRH).

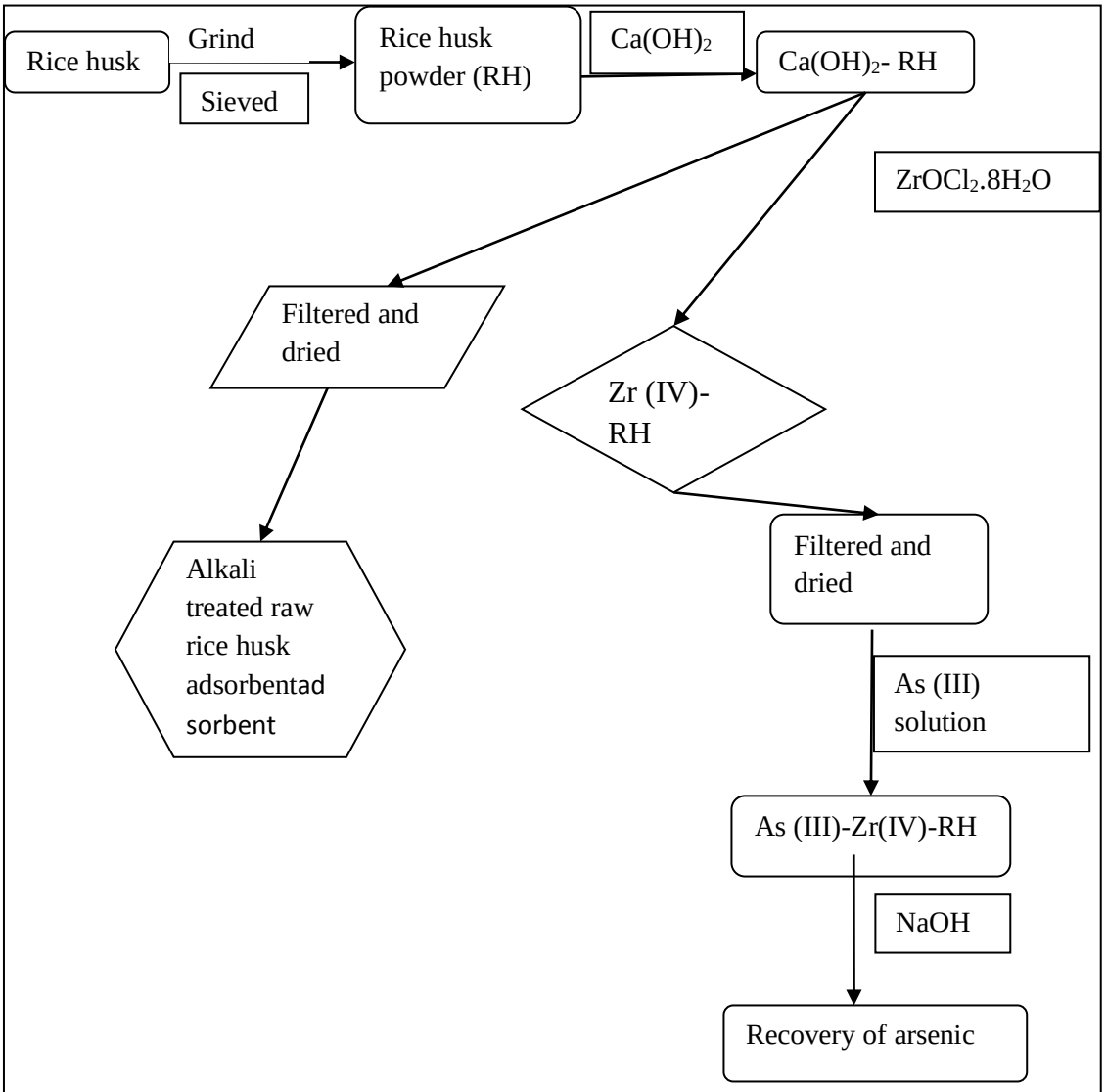

Scheme1: Preparation of adsorbent from rice husk and steps involved in the adsorption process.

3.4.2 Preparation of Zirconium loaded Rice husk adsorbent [Zr(IV)-RH]

20 g of rice husk was treated with 500 mL of a saturated lime solution. The solution was shaken in a mechanical shaker at 190 rpm for 24 hours. The solution was filtered out. The resultant wet product was repeatedly washed with DW by the decantation process still neutral. It was subsequently desiccated for 24 hours at 60°C in a hot air oven. The final yield of rice husk (RH) powder was named $Ca(OH)_2$ saponified rice husk, abbreviated as $Ca(OH)_2$-RH.10 g of $Ca(OH)_2$-RH, was added to a 1.5 M Zr(IV) solution in a conical flask and the flask was shaken for 24 hours. The wet mass was filtered and rinsed numerous times till neutral pH. It was dried in oven at 65^o C for 12h. This process yields a dry powder known as Zr(IV) loaded saponified rice husk, named as Zr(IV)-RH.

3.5 Analytical Part of Adsorption Study

3.5.1 Color Development in As (III) by Molybdenum Blue Method

The spectrophotometric method was utilized to analyze the concentration of As(III), which requires the development of color. The color was developed by adding 5 mL of As (III) sample solution, 4.5 mL of 1.5 N H_2SO_4, 3 mL of 0.1 N $KMnO_4$, 3 mL of 0.5% ammonium molybdate, and 3 mL of 0.5 M hydrazine hydrate in a sequential manner. It was shown through trials that it takes 25 minutes for color to fully develop. The colored solution was then placed in a cuvette, and the spectrophotometer's absorbance was measured.

3.5.2 Determination of λ_{max}

For the determination of maximum wavelength, 2.5 mg/L arsenic solution was made by serial dilution of stock solution. The color was developed using the molybdenum blue method with 5 mL of a 2.5 mg/L arsenic solution. After color development, the absorbance of the solution was examined at various wavelengths between 790 and 890 nm, and the absorbance versus wavelength curve was plotted. The value of the wavelength at which absorbance was at its maximum was taken as the value of λ_{max}.

3.5.3 Construction of Calibration Curve

100 mL of a 2.5 mg/L As (III) solution was made by serially dilution of the stock solution. 0, 1, 2, 3, 4, 5, 6, 7, 8, 9, and 10 mL of this solution were placed in a separate

25 mL VFs. The molybdenum blue method was then used to develop the color. The maximum wavelength was set at 840 nm, and the absorbance of each solution was measured with a spectrophotometer. The plot of absorbance vs. concentration gave a calibration curve.

3.6 Characterization of Adsorbents

The physico-chemical characterization of rice husk was performed by FTIR, SEM, XRD, and EDX. A pH drift method was used to measure potential zero charge (pH_{pzc}).

3.6.1 Instrumental Analysis

SEM-EDX and XRD analysis of the adsorbent was done in the South Korea, FTIR was done at the CDC, Kirtipur.

3.6.2 Determination of pH_{pzc}

The pH_{pzc} of the biosorbent can be evaluated using the pH drift method. NaCl solutions with concentrations of 0.01M, 0.05M, and 0.1M were prepared in a different VF (500 mL). The initial pH of solutions was maintained at pH 1, 2, 3, 4, 5, 6, 7, 8, 9, 10, and 11 using 0.5M HCl and NaOH. 25 mg of Zr(IV)-RH with 20 mL of pH-adjusted 0.01M NaCl solutions was shaken for 24 h. The final pH of the filtrate was analyzed using a pH meter. The difference in pH vs. initial pH was plotted. The same process was repeated for the 0.05M and 0.1M NaCl solutions to obtain the pH_{pzc} of the adsorbent.

3.6.3 Batch Adsorption Study

Adsorption studies were conducted using Zr(IV)-RH to determine the adsorption behavior of As(III).The influence of several influence parameters were studied.25 mg of biosorbent was added to 20 mL of As(III) solution (2 mg/L) in a reagent bottle. The mixture was shaken for 24 hours at room temperature. The equilibrated solution was filtered through filter paper, and the filtrate was used to analyze the residual concentrations of As(III). A spectrophotometer was used to measure the concentrations of As(III) both before and after the adsorption process. The actual concentration of As(III) solution was determined by using the corresponding absorbance value.

3.6.4 Influence of pH

The pH studies were done by shaking 25 mg of biosorbent in 20 mL of the serial solutions of pH 2.0 to 12.0 for 24 h. A mechanical shaker was used to agitate each sample in a reagent bottle. The filtrate was utilized to analyze the residual As (III) concentration. The study compared final concentrations with initial concentrations to determine adsorptive removal percentages. The experiment was performed in triplicate, and mean value was calculated to ensure accuracy and reliability.

3.6.5 Influence of Contact Time

Kinetic tests were performed by adding 25 mg of adsorbents with 20 mL of an arsenite solution of 2mg/L in the reagent bottles at optimum pH. The bottles were subjected to varying durations of shaking in a mechanical shaker, ranging from 1 to 1440 minutes. After that, solutions were filtered at the respective time intervals. Furthermore, the level of As(III) before and after adsorption was analyzed through a spectrophotometer.

3.6.6 Influence of Initial Concentration

Arsenite solutions variable from 0.5 to 400 mg/L were made. 25 mL of each solution were taken in clean, dry stopper bottles to achieve the optimum pH. 5 mL of each adjusted solution were then taken to measure the initial concentration using spectrophotometry. Every bottle was then filled with 25 mg of adsorbent. They were subjected to a 24-hour mechanical shaker set at 190 rpm. Following that, filtration was done, and the filtrate concentration was determined spectrophotometrically. The same data were used to conduct an isotherm study as well.

3.6.7 Influence of Adsorbent Dose

Adsorbents were placed in separate reagent bottles with varying weights ranging from 5 mg to 200 mg. After the pH was optimally adjusted, each of those bottles was filled with 20 mL of 2 mg/L As(III) solutions. The contents were agitated for 24 h. The equilibrated solutions were tested to determine the amount of residual As(III) present.

3.6.8 Influence of Interfering Ions

Various concentrations of phosphate, nitrate, sulfate, and chloride (10, 50, 100, and 200 ppm) were also prepared. 20 mL of As(III) solution was mixed with interfering

ions separately in a different VF(100 mL). The prepared solution was agitated for 24 hours to equilibrate. The influence of these various anions on arsenic's adsorption onto Zr(IV)-RH was investigated and examined using spectrophotometry, as previously mentioned. In 100mL of VFs, As(III) solution (20mL) with interfering anions were prepared separately mixing both solutions.

3.6.9 Batch Desorption Test

100 mg/L As(III) solution was made in a 500mL VF for the desorption experiment, and after maintaining an optimum pH, its initial concentration was determined spectrophotometrically. A prepared As (III) solution was treated with the precisely weighed Zr(IV)-RH (1.202g). It was shaken for 24 hours then filtered, cleaned, and dried. Thus resulting dried sample was termed as As(III) loaded Zr(IV)-RH, abbreviated as As(III)-Zr(IV)-RH. Then, using different concentrations of NaOH as the desorbing solution, the As (III)-Zr(IV)-RH was tested for desorption. Six reagent bottles were filled with 25 mg of As (III)-Zr(IV)-RH for desorption, and 10 mL of NaOH (0.01 M to 1.0 M) was added to each bottle. Subsequently, they were subjected to a 24-hour mechanical shaker. The filtrates after equilibration were subjected to color development and the corresponding absorbance values were noted.

CHAPTER IV

RESULTS AND DISCUSSION

4.1 Evaluation of λ_{max} and Construction of Calibration Curve

4.1.1 Determination of λ_{max}

The λ_{max} was found at 840 nm from the adsorption spectrum of the arsenomolybdenum blue complex in **Figure 2**. All further spectrophotometric measurements were conducted at this wavelength, which was referred to as the "λ_{max}" value. The measured value of (λ_{max}) at 840 nm agrees with the value published by Joshi et al., (2019).

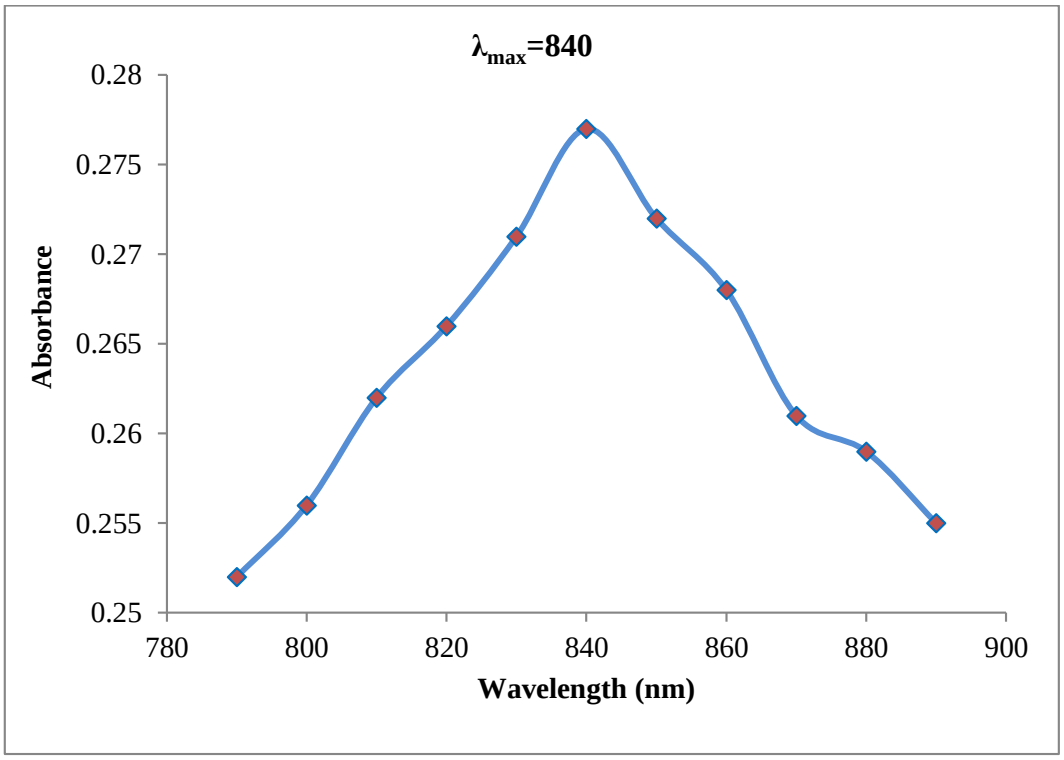

Figure 2: Absorbance plot for arsenomolybdenum blue complex

4.1.2 Construction of Calibration Curve

Maximum absorption was found at 840 nm, hence absorbance values of a series of arsenic solutions of (0.2, 0.4, 0.6, 0.8, 1, 1.2, 1.4, 1.6, 1.8, 2) mg/L were measured at this wavelength specifically. The corresponding plot of absorbance against concentration was found to be linear, indicating that Lambert-Beer's rule is followed.

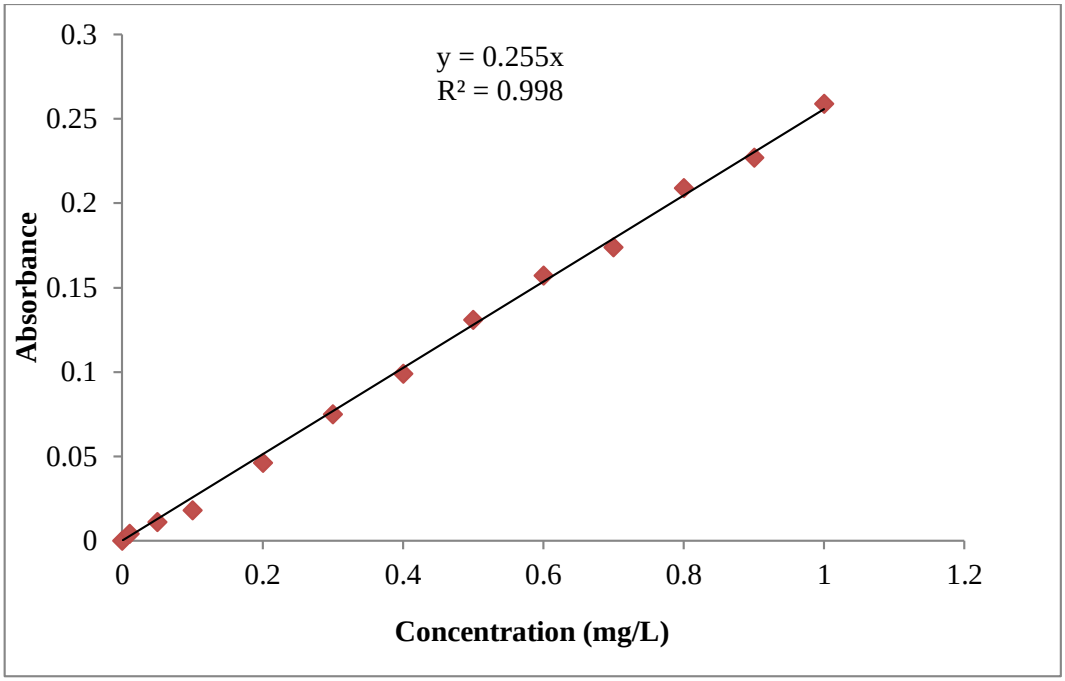

Figure 3: Absorbance vs.concentration

Figure 3 displays that when concentration increases, absorbance also rises linearly, which is due to an increase in the amount of the blue-colored As(III) ion complex. The graph showed a relationship between absorbance and concentration. Using this relationship, the absorbance values were used to calculate the concentration of the desired solutions, provided that all of the reagents included for color development were precisely combined in the same ratio.

4.2 Characterization of Adsorbent

4.2.1 Determination of pH_{PZC}

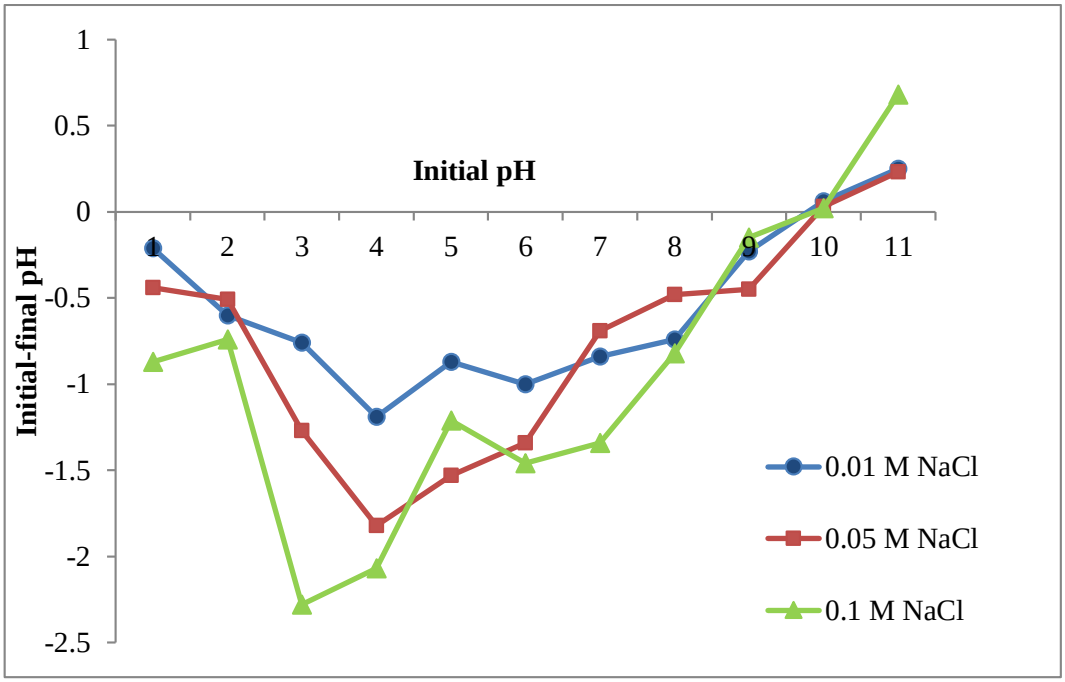

Figure 4: Determination of pHpzc for Zr(IV)-RH

Figure 4 shows the results of pH_{pzc} determination by using NaCl. The pH_{pzc} of Zr (IV)-RH was determined to be 10. At this pH Zr (IV)-RH has no net surface charge. At solution pH less than the pH_{pzc} the surface becomes +vely charged, where the electrostatic force of attraction facilitates the adsorption of anionic species. Therefore, from the result of pH effect, there is rise in biosorption of As (III) below pH_{pzc} value which is at a lower pH value.

4.2.2 FTIR

Figure 5 displays the FTIR spectra of biosorbent before and after arsenic biosorption. Analysis was done on the adsorbents both before and after arsenic adsorption. The broad band seen at around 3600-3200 cm^{-1} is owed to the overlapping of vibrations of the O–H groups and the -NH_2 functional group (Shrestha et al., 2021). Since arsenic and zirconium oxides interacted with a component of the O-H structure, this band shifted to 3408 and 3425 cm^{-1}, respectively (Sheng et al., 2014).

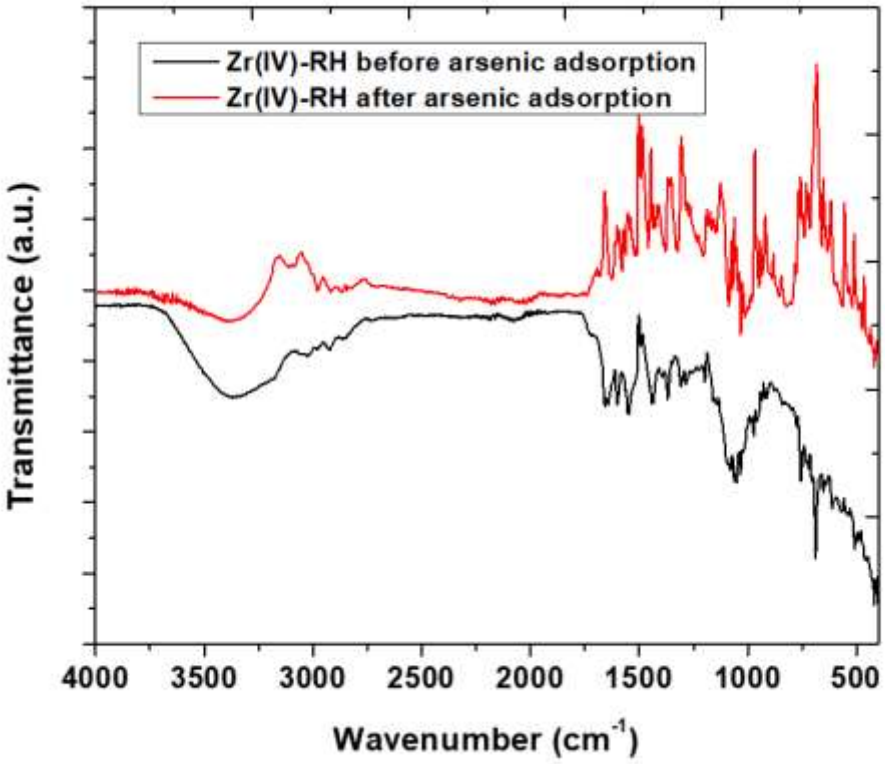

Figure 5: FTIR spectra of biosorbent

Likewise, the next wide band was found at around 2864 cm^{-1}, and it is attributed to the C-H group. The bands at 2331 and 2588 cm^{-1} correspond to either symmetric or asymmetric stretching of the aliphatic band of -CH, $-CH_2$, or $-CH_3$ (Shrestha et al., 2021). More information about the adsorption process was found in the 1200-1800 cm^{-1} range. The carbonyl group was signified by the band at 1700-1900 cm^{-1}, whereas the C-O bond was observed at 1600-1700 cm^{-1}. The stretching vibration of carboxyl groups in Zr(IV)-loaded rice husk gives the bands at 1660 cm^{-1} and 1573 cm^{-1}. These vibrations are moved to 1664 cm^{-1} and 1591 cm^{-1} in arsenic adsorbed Zr(IV)-rice husk. It shows their participation in the adsorption. The peak at 1506 cm^{-1} indicates the C=C stretching in lignin's aromatic ring (Biswas, Inoue et al., 2008a). CH-OH stretching is observed at 1236.37 cm^{-1} (Daffalla et al., 2020). Vibrations of Si-OH stretching were observed at 952 cm^{-1} (Rahim et al., 2015). Bands observed at 470 to 800 cm^{-1} indicate the presence of cyclic siloxanes (Hoyos-Sánchez et al., 2017).

The description above makes it clear that the adsorbent's surfaces are abundant in polymeric -OH and -COOH groups. The primary components of the biosorbent prepared in this work are cellulose and lignin. Additionally, there are other functional

groups that can bind heavy metals to create complexes, such as ether groups, carboxylic acids, alcohols, aldehydes, and phenols.

4.2.3 XRD

XRD patterns of Zr(IV)-RH before and after arsenic biosorption are displayed in **Figures 6** and **7**. XRD pattern of $ZrCa(OH)_2RH$, shows a prominent peak at 2θ value of 22.39º which corresponds to the typical characteristic peak positions of a crystalline form of cellulose. Some of the diffused and weak peaks represent the adsorbent's amorphous structure. According to this, RH is made up of both crystalline and amorphous structures. Zr(IV)-loaded rice husk and As-$ZrCa(OH)_2$-RH retain the same strong peak at 2θ=34º, indicating that only the amorphous area changes when rice husk is modified with Zr(IV) and As(III) is adsorbed.

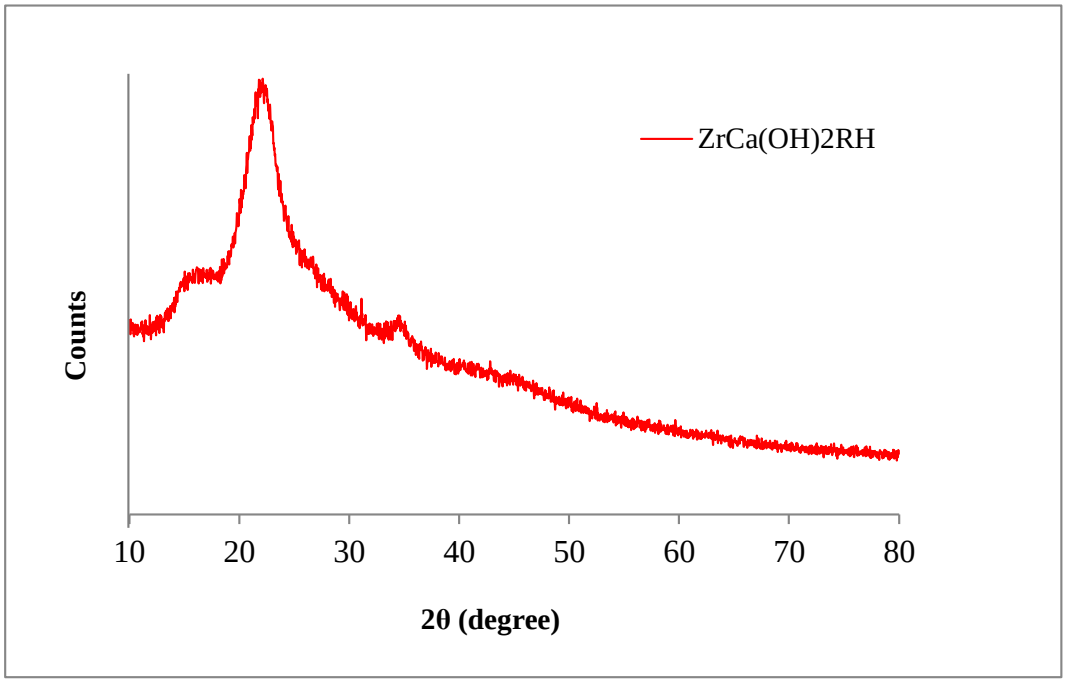

Figure 6: XRD pattern of $ZrCa(OH)_2RH$

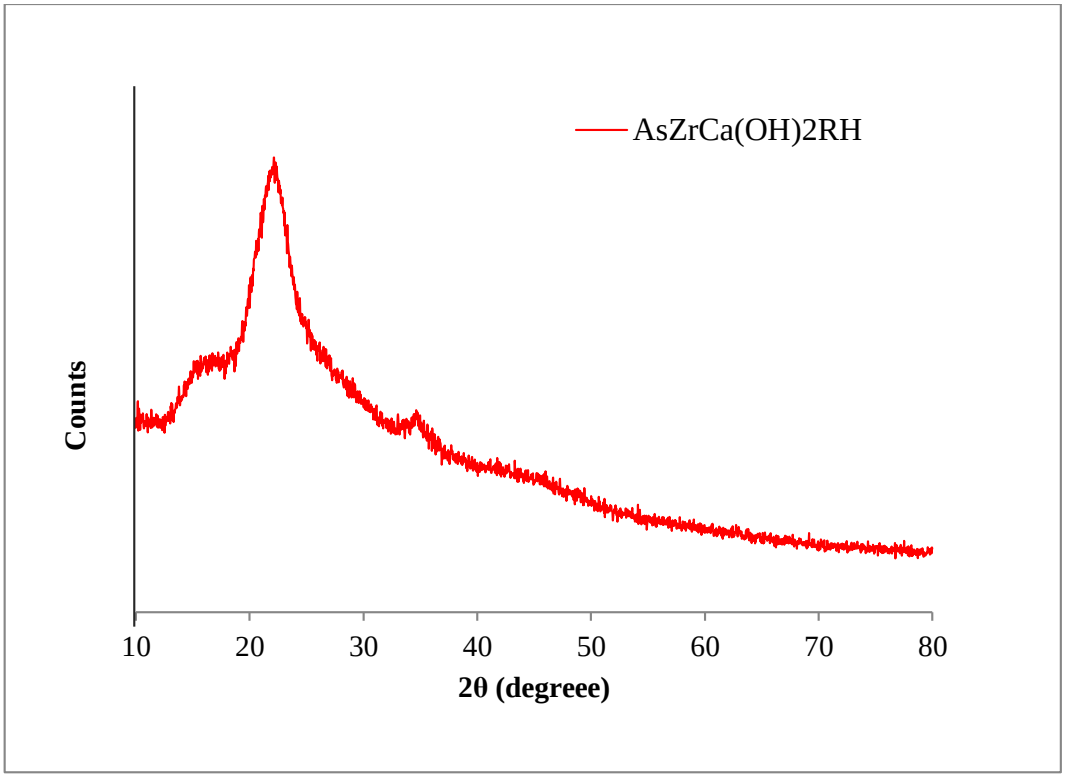

Figure 7: XRD pattern of AsZrCa(OH)$_2$RH

4.2.4 Surface and Elemental Analysis of Adsorbent

The SEM images **(Figure 8)** of Zr(IV)-RH and AsZr(IV)-RH were taken at different magnification to study their morphological characteristics. It was found that treatment of rice husk with a base, improved surface morphology (Daffalla et al., 2020). The figure depicted that the SEM image of Zr(IV)-RH possesses heterogeneous pores with irregular shape. The porous structure increased the surface area of the adsorbent, which is significant for adsorption (Baig et al., 2016).

The surface becomes somewhat smoother in the case of As-Zr(IV)-RH. The surface morphology of As-Zr(IV)-RH changed, and it is reasonable to assume that this was caused by the filling of As(III) on Zr(IV)-RH (Shakoor et al., 2019).

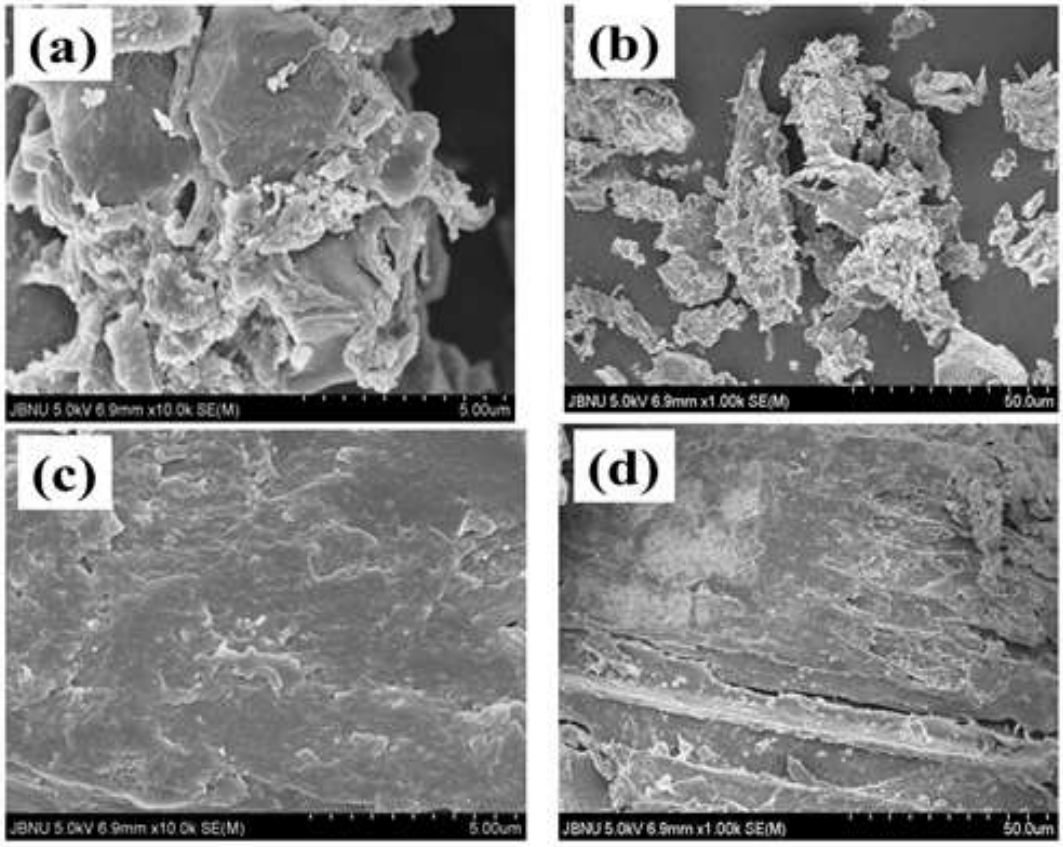

Figure 8: SEM image of Zr(IV)-RH (a, b) and As-Zr(IV)-RH (c, d) at different magnification

4.2.5 EDX Analysis and Elemental Mapping

The adsorbent's chemical composition can be identified using EDX program.

Figure 9(a) and **9(b)** show the EDX spectra of Zr(IV)-RH and As-Zr(IV)-RH, respectively. EDX spectra of Zr(IV)-RH represent the peaks corresponding to the elements Carbon(C), Oxygen(O), Silicon (Mg), and Zirconium (Zr). The EDX spectra of As-Zr(IV)-RH show the peak corresponding to the elements C, O, Si, Zr and As. This indicates that As(III) was adsorbed onto the Zr(IV)-RH.

The EDX layered image in the **Figure 10** shows that the elements are heterogeneously distributed on the biosorbent's surface. Color mapping of the overlapping components detected carbon, oxygen, silicon, and arsenic. It was found that the zirconium rice husk adsorbed arsenic and contained higher amounts of carbon and oxygen, along with 2.9% arsenic.

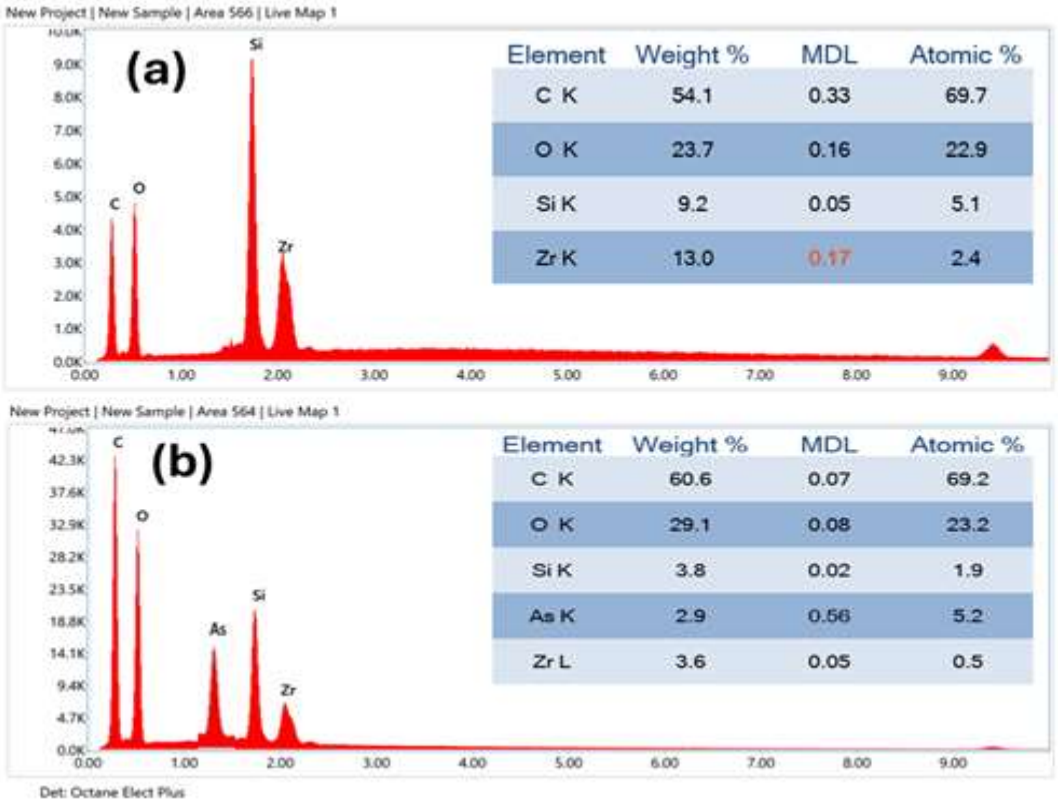

Figure 9: EDX Spectra of (a) Zr(IV)-RH; (b) As-Zr(IV)-RH.

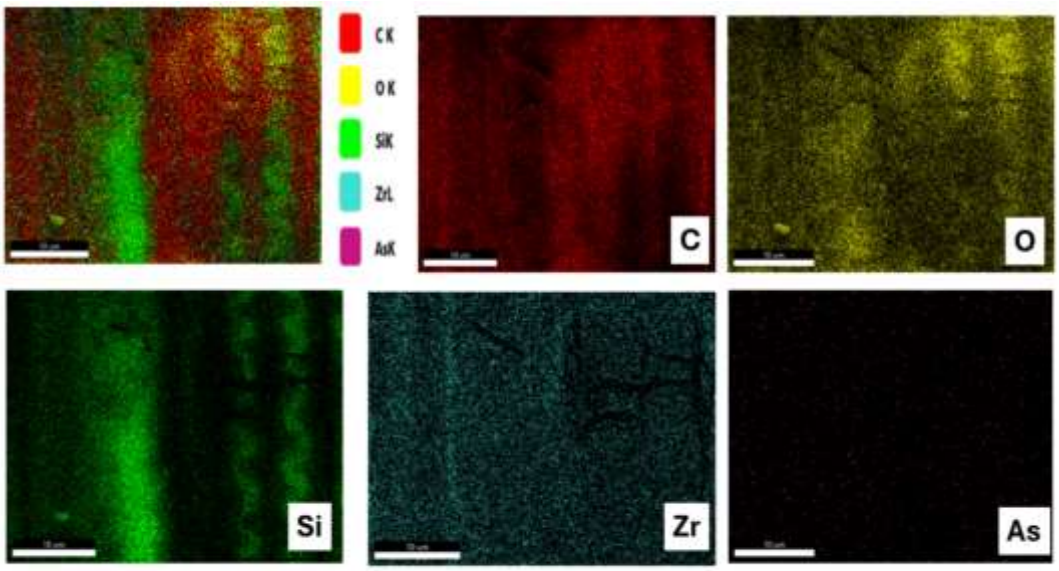

Figure 10: Color mapping images of As adsorbed Zr(IV)-RH.

4.3 Batch Biosorption Process

4.3.1 Influence of pH

The biosorption of ionic adsorbate is affected by the pH of solution because H^+ ions are powerful competitive ions. It affects the sorbent's functional group ionization as well as the sorbate's chemical composition in the solution. As (III) was adsorbed using RH in a variety of pH ranges between 2 and 12, with no chemical modification. **Figure 11** indicates that As(III) adsorption by the raw rice husk is negligible. Thus, it was not convenient to use raw RH as an arsenic removal agent. Therefore, Zr (IV)-RH was used for subsequent testing, and the findings were significantly better than those of raw RH

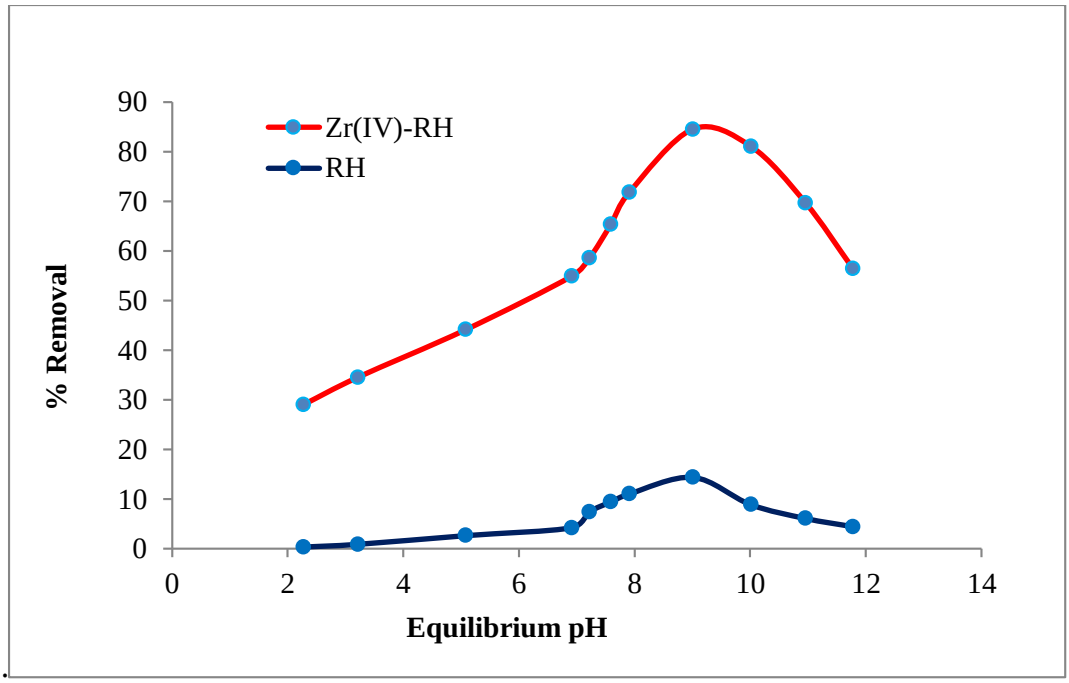

Figure 11: Variation of % adsorption with equilibrium pH of the solution

The arsenic removal percentage at various pH values is displayed using both raw and Zr(IV)-loaded rice husk. This study showed that raising the pH value increased the adsorbent's adsorption capacity. The greatest adsorption efficiency was noted at pH 9. When the pH increased further, the adsorbent's sorption capacity diminished, as seen in **Figure 11**. Less than 12% of As(III) was removed from raw rice husk. However, Zr(IV)-RH displayed a remarkable As(III) removal percentage of up to 85%. (Biswas, Inoue et al., 2008b) determined 10 as the optimum pH in the case of

adsorptive removal of As(III) by Zr(IV)-loaded orange waste gel, which is close to this study.

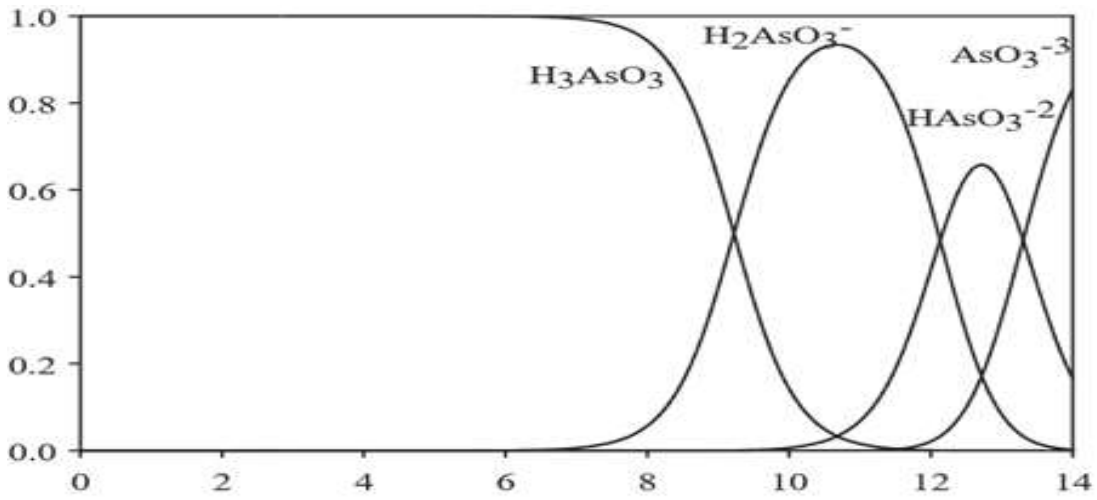

Scheme 2: Distribution of arsenite at various pH values (Aryal et al., 2010).

In a strongly acidic mediumAs(III) mostly occurs as a neutral H_3AsO_3 species, and the biosorbent surfaces are exceedingly protonated, subsequently biosorption is unfavorable. Anionic species ($H_3AsO_3^-$ and $HAsO_3^-$) can be formed when H_3AsO_3 deprotonates at pH values between 7 and 9. The +vely charged biosorbent surface attracts the negatively charged $H_2AsO_3^-$ and $HAsO_3^{2-}$. At this pH range, As (III) absorption is high. Arsenic(III) was adsorbed onto the adsorbent surface by replacing the water molecules or hydroxyl ions that were initially attached to the loaded Zr(IV) ion (Joshi et al., 2019).

Adsorption mechanism of arsenic removal

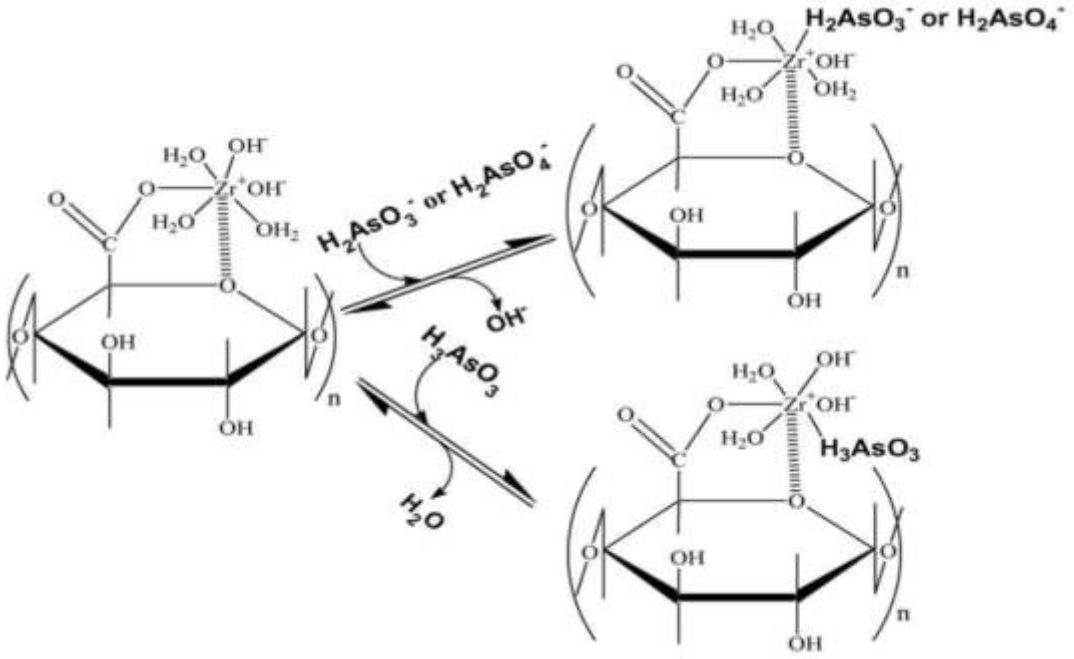

Scheme 3: [As(III) adsorption mechanism] (Biswas, Inoue, et al., 2008b)

Arsenite anions and neutral H_3AsO_3 molecule replace hydroxyl ions or coordinated H_2O molecules in the adsorption mechanism described above.

4.3.2 Influence of Contact Time

The duration of interaction between adsorbate and adsorbent affects the adsorption capacity. As the contact time increases, the biosorption significantly increase still it scopes the equilibrium point. Once the equilibrium time is reached, there is no considerable increase in adsorption rate because adsorption sites get almost full.

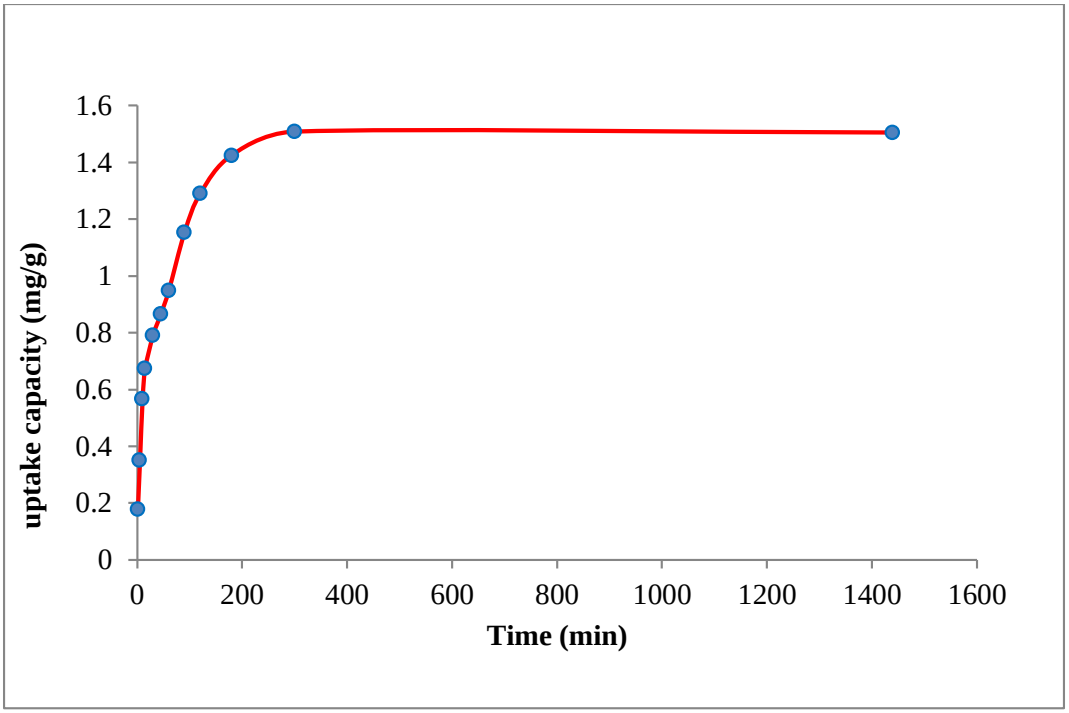

Figure 12: Variation of the As(III) uptake capacity onto Zr(IV)-RH vs. time.

Figure 12 displays the equilibrium contact time for As(III) removal on Zr(IV)-RH is 5 hours. In the initial stages, the adsorption rate was higher because there were many active sites. The active sites are becoming more and more saturated with As (III) ions over a period of time. Following this, the adsorption rate gradually decreased until it attained adsorption equilibrium. Consequently, it is shown that the biosorption rate is directly related to the number of accessible adsorption sites. Even though equilibrium was reached in 5 hours, further work was done for 24 hours to make sure the equilibrium was completely reached.

4.3.3 Kinetic Modeling

The experiment was analyzed using PFO and PSO kinetic models to identify the top fitting kinetic model and evaluate the adsorption mechanism. The plot of "log(qe-qt)" vs. "time" is displayed by the PFO model, and the plot of "t/qt" versus "time" is displayed by the PSO model.

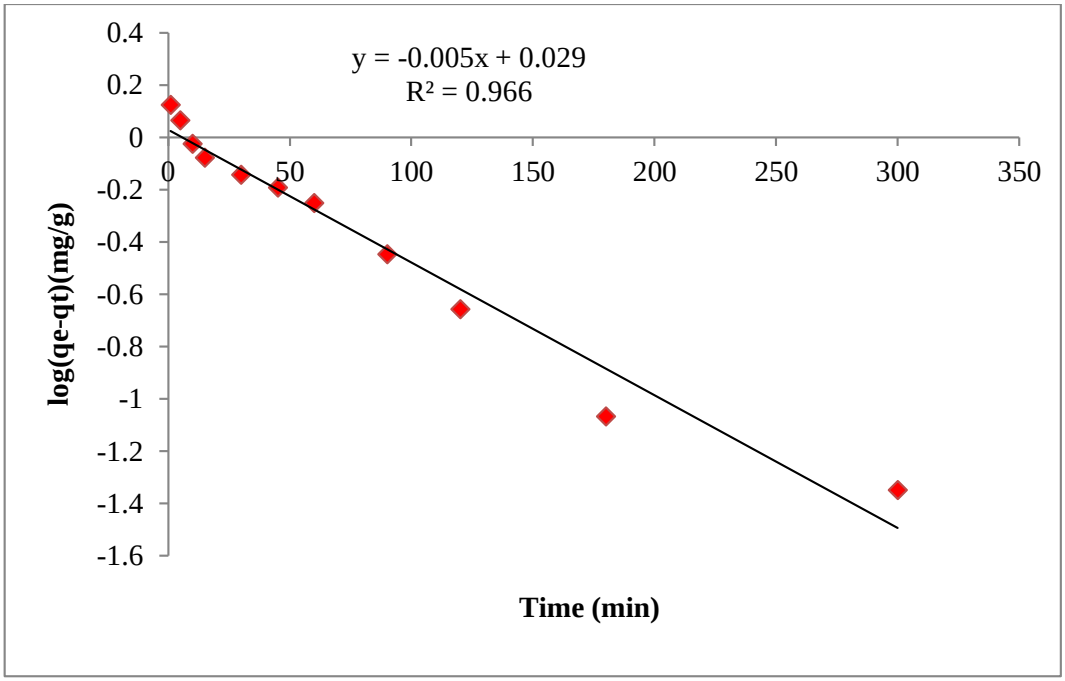

Figure 13: PFO kinetic plot

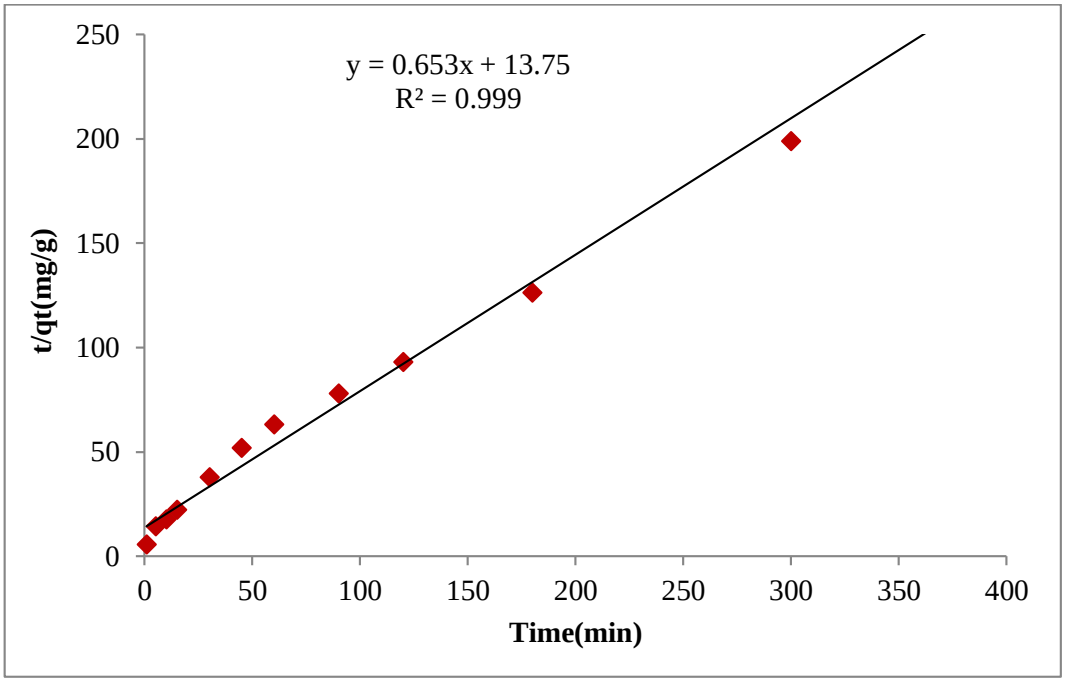

Figure 14: PSO kinetic plot

The plots of PFO and PSO models generated the straight lines. However PSO kinetics has a higher R^2 value than PFO kinetics.

Table 3: Kinetic parameters of biosorption of As(III) onto Zr(IV)-RH

Species	**Adsorbent**	**Experimental qe (mg/g)**	**Pseudo-first-order kinetic model**			**Pseudo-second-order kinetic model**		
As (III)	Zr(IV)-RH	1.508	K_1(min^{-1})	qe (mg/g)	R^2	K_2 ($gmg^{-1}min^{-1}$	qe (mg/g)	R^2
			0.011	1.069	0.817	0.170	1.531	0.999

Based on the qe value, the kinetic modeling of every adsorption was explained in the above table. When the qe values of both orders were compared, the PSO value agreed more closely with the experimentally determined qe value. According to the PSO model, the As(III) uptake capacity is 1.531 mg/g, whereas the PFO model yields 1.069 mg/g. Therefore, it can be resolved that the kinetic behavior of the biosorption is better predicted by PSO and chemisorptions is the rate-determining step (Agrafioti et al., 2014).

4.3.4 Influence of Concentration of As(III) Solution

It demonstrates that adsorption increases with increasing initial concentration of As(III) and reaches equilibrium since there are limited sorption sites available. It indicates that the biosorption trails the Langmuir isotherm. As arsenic concentration increases the mass transfer driving forces are enhanced. It accelerates the movement of As(III) anions from bulk solution to the surface of biosorbent and leads to increased adsorption. After equilibrium, there is a gradual decrease in percentage removal due to the decline in the adsorptive surface and ions competition for available binding sites on the adsorbent.

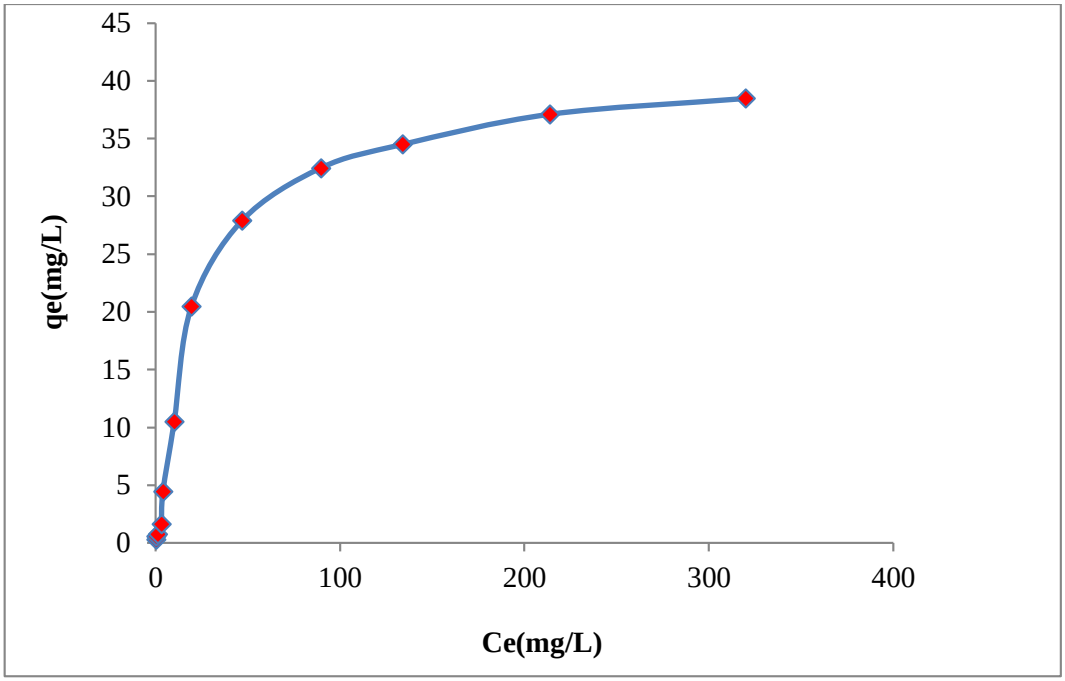

Figure 15: Variation of adsorption capacity of Zr(IV)-RH with equilibrium concentration

4.3.5 Isotherm Modeling

The Langmuir isotherm using data of 'Ce/qe' vs. 'Ce' (**Figure 16**) and the Freundlich isotherm was plotted using 'logqe' vs. 'logCe '(**Figure 17**) The linear Freundlich and Langmuir equations were plotted, to predict the correlation coefficients and related constants. The Langmuir model was considered as the better suited model due to its high correlation coefficients. **Table 4** contains the evaluation results for the isotherm parameters. The Langmuir equilibrium parameter (K_L) was found to be 0.02 L/mg, while the Freundlich model's 1/n value was 0.67, which indicates the adsorption process is favorable. A Langmuir model was utilized to determine q_{max} of As(III) onto Zr(IV)-RH which is 43.47 mg/g. This q_{max} value closely matches the 38.45 mg/g adsorption capacity found in the plateau region of the isotherm curve.

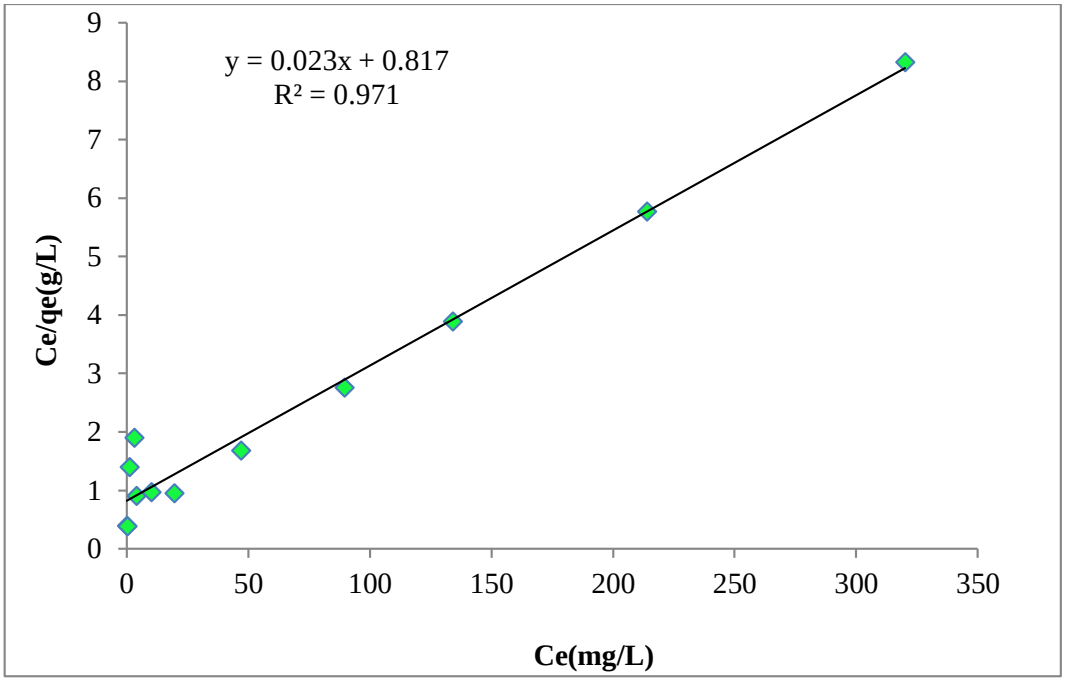

Figure 16: Langmuir adsorption isotherm plot

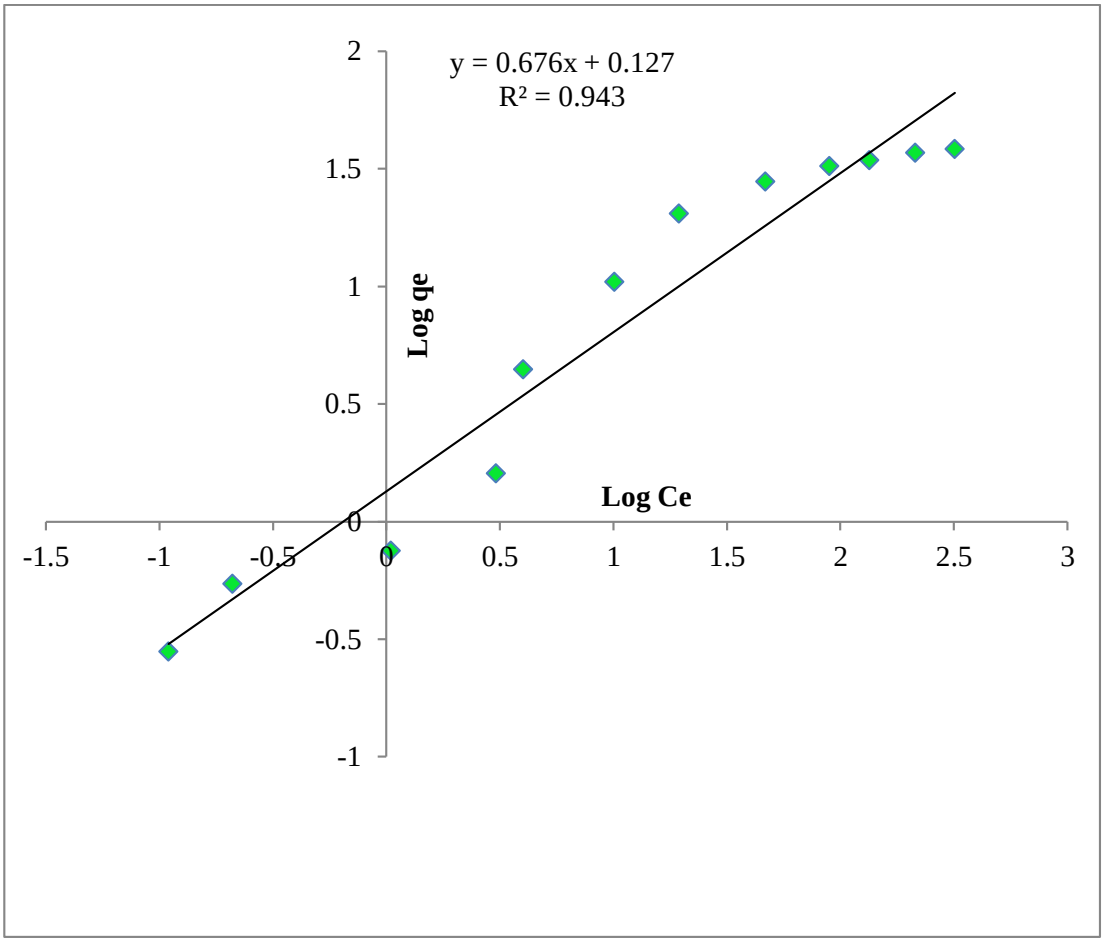

Figure 17: Freundlich adsorption isotherm plot

Table 4: Isotherm parameters for adsorption of As(III) onto Zr(IV)-RH

Species	**Adsorbent**	**q_m exptl. maxima (mg/g)**	**Langmuir isotherm**			**Freundlich isotherm**		
As(III)	Zr(IV)-RH	38.45	qm (mg/g)	K_L (L/mg)	R^2	K_f (mg/g)	1/n	R^2
			43.47	0.02	0.97	1.34	0.67	0.94

Another method for identifying the favorability of the adsorption process is to calculate R_L, as follows,

$$R_L = \frac{1}{1+K_L C_i} \text{.....(xiii)}$$

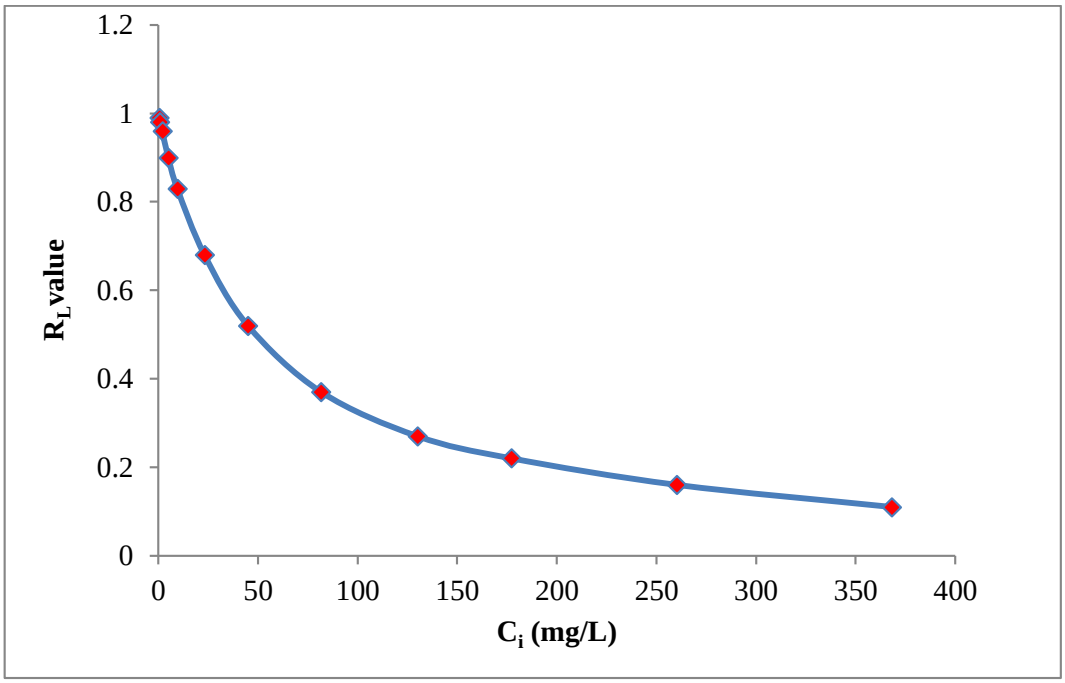

Figure 18: A plot of R_L vs. C_i for adsorption of As(III) onto Zr(IV)-RH

A graph plotted above shows the calculated R_L value against all of the initial concentrations that were taken. It shows that the adsorption process is very beneficial because all the R_L values fell 0 to 1.

The q_{max} of Zr(IV)-RH, and other adsorbents that have been previously studied by other researchers, are listed in **Table 5** for comparison.

Table 5: Comparison of q_{max} of Zr(IV)-RH along with various adsorbents.

S.N.	Adsorbents	q_{max}(mg/g)	References
1	Fe(III) loaded sugarcane bagasse	25	(Chand et al., 2015)
2	AC composite	6.69	(Joshi et al., 2019)
3	Zirconium polyacrylamide hybrid material	41.48	(S. Mandal et al., 2013)
4	Zirconium modified pomegranate peel	72.52	(Poudel et al., 2022)
5	Iron-coated honeycomb briquette cinders	0.96	(Sheng et al., 2014)
6	Zirconium loaded SOW gels	130	(Biswas, Inoue, et al., 2008b)
7	Magnetic bleached biochar	18.86	(McGeogh et al., 2024)
8	Kigelia Africana carbons	84.21	(Yadav et al., 2019)
9	Oak wood char	4.93	(Mohan et al., 2011)
10	Zr(IV)- Rice Husk	43.47	Present work

4.3.6 Influence of Adsorbent Dose

Figure 19 displays the Influence of biosorbent dose on As biosorption. The arsenic removal was found to increase as the adsorbent dosage augmented. This is because there are more active sites and a larger surface area at higher dosages. After equilibrium, more addition did not alter in the removal of arsenic. This happens when adsorption site aggregation leaves the adsorbent with no active sites remaining.

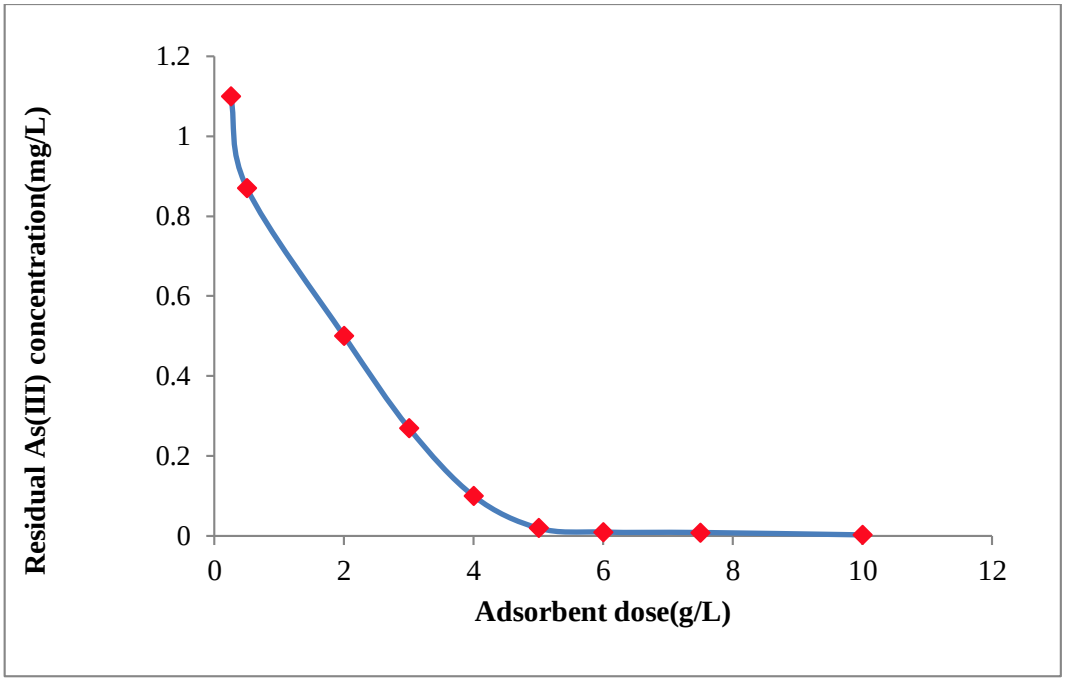

Figure 19: Variation of residual concentration of As(III) with adsorbent

According to the figure, the C_o of 2 mg/L As(III) is lowered to 100% at an adsorbent dose of 5 g/L or higher. It is sufficient to lower the As(III) amount down to WHO standard (10µg/L). Therefore, it can be assumed that the Zr(IV)-RH will be an effective substance for removing As(III) residues from arsenic-contaminated water.

4.3.7 Influence of Interfering Ions

The water may contain several anions. In this study, the main interfering ions, such as silicate, nitrate, sulfate, and phosphate, have been investigated. The initial concentration of As(III) was maintained at 1.22 mgL^{-1}, whereas the concentration of anions was varied between 10 mgL^{-1} and 200mg L^{-1}.

It has been noted that the biosorption process is slowed down in the presence of interfering ions. The order in which the biosorption decrease by anions is given as follows: Phosphate> Sulfate> Silicate > Nitrate (Biswas, Inoue et al., 2008; Nicomel et al., 2016). Phosphate exhibits the greatest interference among all four anions in the adsorption, resulting in a decline in the removal rate from 86.88% to 58.19%.

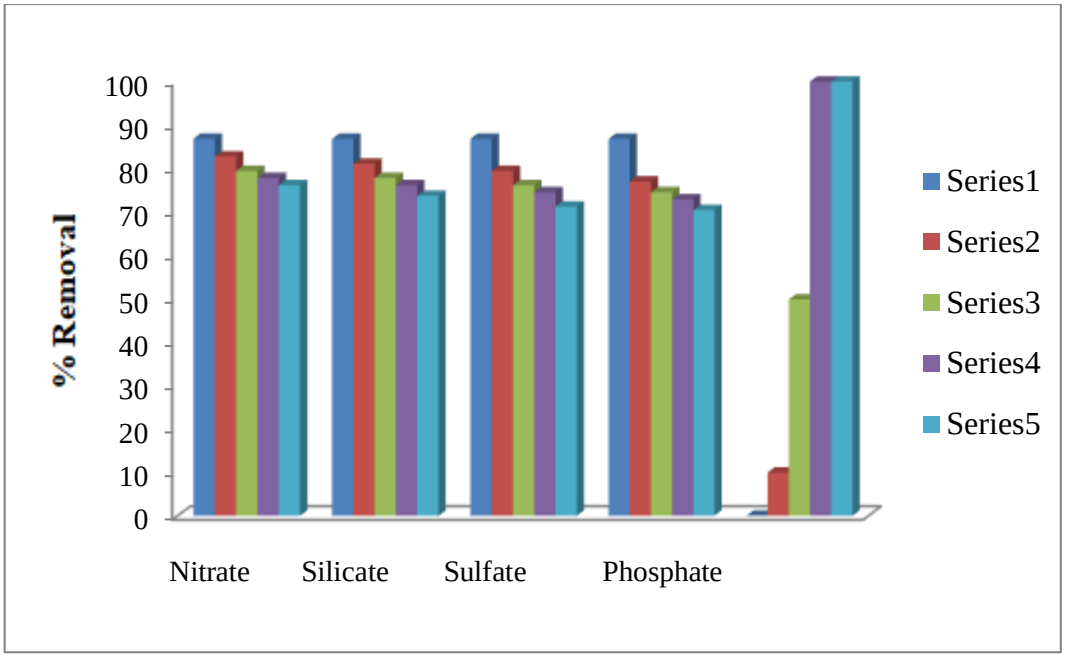

Figure 20: Influence of interfering ion on the elimination of As(III) by Zr(IV)-RH

This lessening in biosorption capacity may be owing to these ions competing with the arsenic for the available sorption sites. Additionally, the affinity of these anions for the adsorbent material could also contribute to their impact on adsorption (Mandal et al., 2013). The phosphate anion had a larger affinity for the adsorbent than the other anion, so it may have caused the strongest interference. However, it is clear that, out of all the interfering ions, arsenite anions showed the greatest affinity with absorbent.

4.3.8 Desorption Studies

A problem might arise with the disposal of contaminated waste biosorbent. Desorption experiments are therefore essential for examining a biosorbent's potential for recycling. After desorption test regenerated biosorbent RH is risk free to dispose since it does not contain any heavy metal.

Eluents such as NaOH, NaCl, and HCl are commonly used in the analysis of desorption experiments. When the influence of interfering anions was studied, Cl^- ion generated by NaCl had the least interaction with adsorptive removal. It was thought that Cl^- ion might not be able to effectively desorb arsenite anions because it has a lower affinity with the prepared adsorbent. Therefore, desorption was performed using 0.01 M to 2M NaOH solution. The study of the pH effect found that the optimum pH was 9. It suggests that at pH >9, the biosorption of arsenite anion is less favorable.

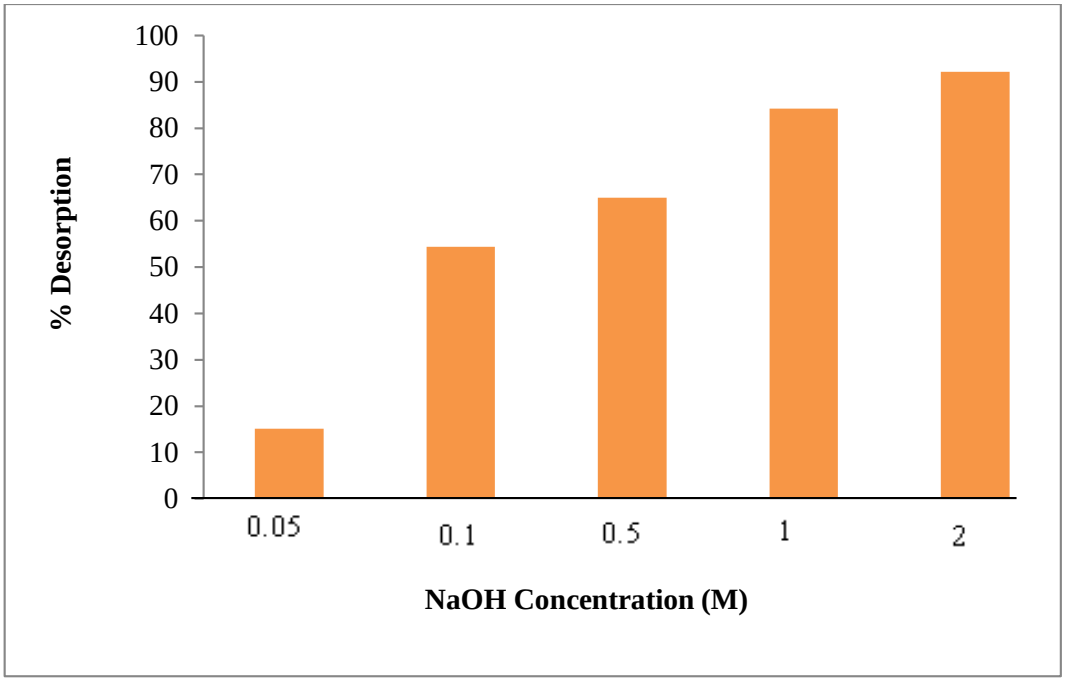

Figure 21: Desorption percentage of As(III) vs. molar concentration of NaOH.

Figure 21 displays the desorption percentage of adsorbed arsenite anion vs. concentration of NaOH. When the concentration of NaOH is raised from 0.01M to 2M, the desorption percentage of As(III) increases. Thus, 92.21% effective desorption was accomplished with a 2M NaOH. This suggests that Zr(IV)-RH's potential for regeneration makes it a valuable adsorbent for the following cycle.

The As(III) desorption mechanism may be described by the ligand exchange mechanism as illustrated in **Scheme 4.** When the arsenite solution is treated with NaOH solution, the pH level increases. Thus, there is repulsion between the hydroxyl ion and the arsenite anion. As a result, the hydroxyl group replaces the arsenite anion, which causes the arsenite anion to desorb.

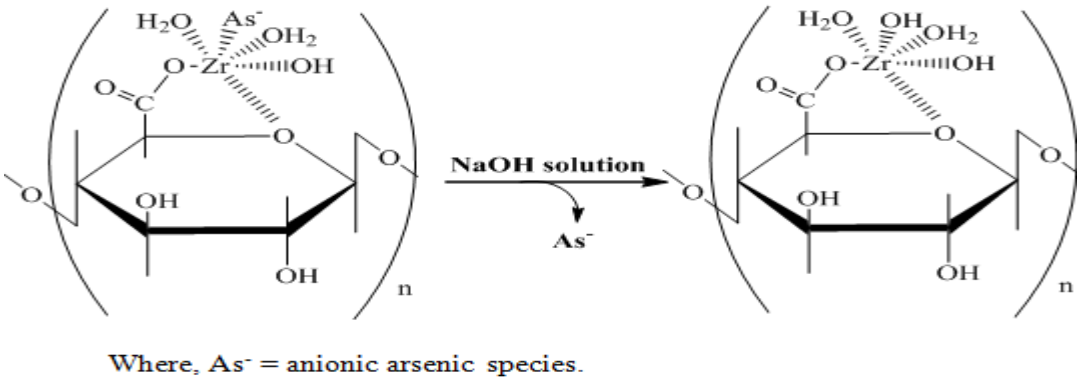

Where, As^- = anionic arsenic species.

Scheme 4: Mechanism of As(III) desorption using NaOH solution (Poudel et al., 2022)

CHAPTER V

CONCLUSION

The Zr(IV)-RH was prepared and characterized. According to the study, Zr(IV)-RH is a significantly better adsorbent than raw rice husk. As(III) biosorption is remarkably pH-dependent, and q_{max} occurs at pH 9. The PSO model and the Langmuir model both fit perfectly with the experimental results. The q_{max} of Zr(IV)-RH for As(III) from was estimated to be 43.47 mg/g which is very close to the experimental adsorption capacity 38.45 mg/g. The studies were conducted over a 24-hour period to guarantee perfect equilibrium, even though the effective contact time was just 5 hours at a speed of 190 rpm. The pH_{pzc} of the Zr(IV)-RH is found to be 10. Interfering anions like nitrate, sulfate, and silicate slightly suppress the adsorbent's As(III) uptake capacity, while phosphate significantly interferes with the adsorption process. Sodium hydroxide is employed as an eluent in the desorption test at different concentrations (0.01M-2M). According to the results, 2M NaOH has a higher desorption percentage (92.21%). In conclusion, this study shows that Zr(IV)-RH, an adsorbent prepared from rice husk, is a suitable substance for eliminating As(III) from aqueous solution.

5.1 Limitation of the Study

1. The experiment was done simply using laboratory-grade chemicals.
2. Characterization methods such as TEM, XPS, and XRF were not used. Not all adsorbent modifications could be easily achieved with the available techniques, namely EDX, FTIR, SEM, and XRD.
3. Study of variables like the influence of agitation, temperature and speed has not been done.
4. There was no column study conducted.
5. There were no further possible eluents used in the elution trial; only NaOH solution was used as an eluent.
6. The whole experiment was carried out in a laboratory condition.

5.2 Recommendation for further Study

- Adsorbent structural characteristics can be demonstrated by characterization techniques including XPS, XRF, and TEM.
- The study of variables such as temperature and the impact of agitation speed can be included in the research.
- Regeneration potential of Zr(IV)-RH and As(III) recovery can be investigated.
- The experiment can be carried out in column mode.

REFERENCES

Agrafioti, E., Kalderis, D., &Diamadopoulos, E. (2014). Arsenic and chromium removal from water using biochars derived from rice husk, organic solid wastes and sewage sludge. *Journal of environmental management*, *133*, 309-314.

Ali, I., & Gupta, V. K. (2006). Advances in water treatment by adsorption technology. *Nature protocols*, *1*(6), 2661-2667.

Al-Rashdi, B., Somerfield, C., &Hilal, N. (2011). Heavy Metals Removal Using Adsorption and Nanofiltration Techniques.*Separation & Purification Reviews*, *40*(3), Article 3.

Amin, M. N., Kaneco, S., Kitagawa, T., Begum, A., Katsumata, H., Suzuki, T., &Ohta, K. (2006). Removal of arsenic in aqueous solutions by adsorption onto waste rice husk. *Industrial & Engineering Chemistry Research*, *45*(24), 8105-8110.

Aryal, M., Ziagova, M., & Liakopoulou-Kyriakides, M. (2010). Study on arsenic biosorption using Fe (III)-treated biomass of Staphylococcus xylosus. *Chemical Engineering Journal*, *162*(1), 178-185.

Asif, Z., & Chen, Z. (2017a). Removal of arsenic from drinking water using rice husk. *Applied Water Science*, *7*, 1449-1458.

Asif, Z., & Chen, Z. (2017b). Removal of arsenic from drinking water using rice husk. *Applied Water Science*, *7*(3), 1449–1458.

Atkins, P. W., & Paula, J. de. (2014). *Atkins' Physical Chemistry*. OUP Oxford.

.Bakatula, E. N., Richard, D., Neculita, C. M., &Zagury, G. J. (2018). Determination of point of zero charge of natural organic materials. *Environmental Science and Pollution Research*, *25*, 7823-7833.

Baig, J. A., Kazi, T. G., Shah, A. Q., Kandhro, G. A., Afridi, H. I., Khan, S., & Kolachi, N. F. (2010). Biosorption studies on powder of stem of Acacia nilotica: removal of arsenic from surface water. *Journal of hazardous materials*, *178*(1-3), 941-948.

Biswas, B. K., Inoue, J., Inoue, K., Ghimire, K. N., Harada, H., Ohto, K., &Kawakita, H. (2008a). Adsorptive removal of As(V) and As(III) from water by a Zr(IV)-loaded orange waste gel. *Journal of Hazardous Materials*, *154*(1), 1066–1074.

Biswas, B. K., Inoue, J., Inoue, K., Ghimire, K. N., Harada, H., Ohto, K., &Kawakita, H. (2008b). Adsorptive removal of As(V) and As(III) from water by a Zr(IV)-loaded orange waste gel. *Journal of Hazardous Materials*, *154*(1–3), 1066–1074.

Chand, T. H., Raj, P. M., Nath, G. K., &Bahadur, K. D. (2015). Removal of arsenic from aqueous solution using iron (III)-loaded sugarcane bagasse. *Research Journal of Chemical Sciences*.

Chaudhry, S. A., Khan, T. A., & Ali, I. (2017). Zirconium oxide-coated sand based batch and column adsorptive removal of arsenic from water: isotherm, kinetic and thermodynamic studies. *Egyptian journal of petroleum*, *26*(2), 553-563.

Chowdhury, S., Misra, R., Kushwaha, P., & Das, P. (2011). Optimum sorption isotherm by linear and nonlinear methods for safranin onto alkali-treated rice husk. *Bioremediation Journal*, *15*(2), 77-89.

Cuong, D. V., Wu, P. C., Liou, S. Y. H., &Hou, C. H. (2022). An integrated active biochar filter and capacitive deionization system for high-performance removal of arsenic from groundwater. *Journal of Hazardous Materials*, *423*, 127084.

Daffalla, S. B., Mukhtar, H., &Shaharun, M. S. (2020). Preparation and characterization of rice husk adsorbents for phenol removal from aqueous systems. *PloS one*, *15*(12), e0243540.

Dhakal, R. P., Ghimire, K. N., & Inoue, K. (2005). Adsorptive separation of heavy metals from an aquatic environment using orange waste. *Hydrometallurgy*, *79*(3-4), 182-190.

Fiol, N., &Villaescusa, I. (2009). Determination of sorbent point zero charge: usefulness in sorption studies. *Environmental chemistry letters*, *7*, 79-84.

Guo, X., & Wang, J. (2019). Comparison of linearization methods for modeling the Langmuir adsorption isotherm. *Journal of Molecular Liquids*, *296*, 111850.

Hoyos-Sánchez, M. C., Córdoba-Pacheco, A. C., Rodríguez-Herrera, L. F., & Uribe-Kaffure, R. (2017). Removal of Cd (II) from Aqueous Media by Adsorption onto Chemically and Thermally Treated Rice Husk. *Journal of Chemistry*, *2017*, e5763832.

Hughes, M. F., Beck, B. D., Chen, Y., Lewis, A. S., & Thomas, D. J. (2011). Arsenic Exposure and Toxicology: A Historical Perspective. *Toxicological Sciences*, *123*(2), Article 2.

Ismail, A. A., van de Voort, F. R., &Sedman, J. (1997). Fourier transform infrared spectroscopy: principles and applications. In *Techniques and instrumentation in analytical chemistry* (Vol. 18, pp. 93-139). Elsevier.

Javed, K., Mahmood, S., Ammar, M., Abbas, N., Shah, M. Y., Ahmed, T., & Mustafa, G. (2023). Rice husk ash adsorbent modified by iron oxide with excellent adsorption capacity for arsenic removal from water. *International Journal of Environmental Science and Technology*, *20*(3), 2819-2828.

John, Y., David, V. E., &Mmereki, D. (2018). A comparative study on removal of hazardous anions from water by adsorption: a review. *International Journal of Chemical Engineering*, *2018*.

Jones, F. T. (2007). A broad view of arsenic. *Poultry science*, *86*(1), 2-14.

Joshi, S., Sharma, M., Kumari, A., Shrestha, S., & Shrestha, B. (2019). Arsenic removal from water by adsorption onto iron oxide/nano-porous carbon magnetic composite. *Applied Sciences*, *9*(18), 3732.

Kalam, S., Abu-Khamsin, S. A., Kamal, M. S., &Patil, S. (2021). Surfactant adsorption isotherms: A review. *ACS omega*, *6*(48), 32342-32348.

Kamsonlian, S., Suresh, S., Ramanaiah, V., Majumder, C. B., Chand, S., & Kumar, A. (2012). Biosorptivebehaviour of mango leaf powder and rice husk for arsenic (III) from aqueous solutions. *International Journal of Environmental Science and Technology*, *9*, 565-578.

Lee, C. K., Low, K. S., Liew, S. C., &Choo, C. S. (1999). Removal of arsenic (V) from aqueous solution by quaternized rice husk. *Environmental Technology*, *20*(9), 971-978.

Lee, K. S., Shim, H. Y., Lee, D. S., & Chung, D. Y. (2015). The fate and factors determining arsenic mobility of arsenic in soil-A review. *Korean Journal of Soil Science and Fertilizer*, *48*(2), 73-80.

Mandal, B. K., & Suzuki, K. T. (2002). Arsenic round the world: a review. *Talanta*, *58*(1), 201-235.

Mandal, S., Sahu, M. K., & Patel, R. K. (2013). Adsorption studies of arsenic (III) removal from water by zirconium polyacrylamide hybrid material (ZrPACM-43). *Water resources and industry*, *4*, 51-67.

McGeogh, M., Annath, H., &Mangwandi, C. (2024). Turning teawaste particles into magnetic bio-sorbents particles for arsenic removal from wastewater: Isotherm and kinetic studies. *Particuology*, *87*, 179-193.

Mohammed, A., & Abdullah, A. (2018, November). Scanning electron microscopy (SEM): A review. In *Proceedings of the 2018 International Conference on Hydraulics and Pneumatics—HERVEX, BăileGovora, Romania* (Vol. 2018, pp. 7-9).

Mohan, D., Rajput, S., Singh, V. K., Steele, P. H., & Pittman Jr, C. U. (2011). Modeling and evaluation of chromium remediation from water using low cost bio-char, a green adsorbent. *Journal of hazardous materials*, *188*(1-3), 319-333.

Mondal, M. K., &Garg, R. (2017). A comprehensive review on removal of arsenic using activated carbon prepared from easily available waste materials. *Environmental Science and Pollution Research*, *24*, 13295-13306.

Montalvo-Andía, J., Reátegui-Romero, W., Peña-Contreras, A. D., Zaldivar Alvarez, W. F., King-Santos, M. E., Fernández-Guzmán, V., ... &Mondal, M. K. (2022). Adsorption of Cd (II) using chemically modified rice husk: characterization, equilibrium, and kinetic studies. *Adsorption Science & Technology*, *2022*, 1-17.

Nicomel, N. R., Leus, K., Folens, K., Van Der Voort, P., & Du Laing, G. (2016). Technologies for arsenic removal from water: current status and future perspectives. *International journal of environmental research and public health*, *13*(1), 62.

Nguyen, T. A. H., Ngo, H. H., Guo, W. S., Zhou, J. L., Wang, J., Liang, H., & Li, G. (2014). Phosphorus elimination from aqueous solution using 'zirconium loaded okara'as a biosorbent. *Bioresource technology*, *170*, 30-37.

Parascandola, J. (2012). *King of poisons: a history of arsenic*. Potomac Books, Inc.

Pehlivan, E., Tran, T. H., Ouédraogo, W. K. I., Schmidt, C., Zachmann, D., &Bahadir, M. (2013). Removal of As (V) from aqueous solutions by iron coated rice husk. *Fuel processing technology*, *106*, 511-517.

Pillai, P., Kakadiya, N., Timaniya, Z., Dharaskar, S., & Sillanpaa, M. (2020). Removal of arsenic using iron oxide amended with rice husk nanoparticles from aqueous solution. *Materials Today: Proceedings*, *28*, 830-835.

Poudel, B. R., Ale, D. S., Aryal, R. L., Ghimire, K. N., Gautam, S. K., Paudyal, H., &Pokhrel, M. R. (2022). Zirconium modified pomegranate peel for efficient removal of arsenite from water. *BIBECHANA*, *19*(1-2), 1-13.

Qu, S., Wu, G., Fang, J., Zang, D., Xing, H., Wang, L., & Wu, H. (2017). Dielectric and magnetic loss behavior of nanooxides. In *Spectroscopic Methods for Nanomaterials Characterization* (pp. 301-319). Elsevier.

Rahidul Hassan, H. (2023). A review on different arsenic removal techniques used for decontamination of drinking water. *Environmental Pollutants and Bioavailability*, *35*(1), 2165964.

Rahim, M. A. A., Ismail, M. M., &Mageed, A. M. A. (2015). Production of activated carbon and precipitated white nanosilica from rice husk ash,". *International Journal of Advanced Research*, *3*(2), 491-498.

Saadi, R., Saadi, Z., Fazaeli, R., &Fard, N. E. (2015). Monolayer and multilayer adsorption isotherm models for sorption from aqueous media. *Korean Journal of Chemical Engineering*, *32*, 787-799.

Scimeca, M., Bischetti, S., Lamsira, H. K., Bonfiglio, R., &Bonanno, E. (2018). Energy Dispersive X-ray (EDX) microanalysis: A powerful tool in biomedical research and diagnosis. *European journal of histochemistry: EJH*, *62*(1).

Shakoor, M. B., Niazi, N. K., Bibi, I., Shahid, M., Saqib, Z. A., Nawaz, M. F., ...&Rinklebe, J. (2019). Exploring the arsenic removal potential of various biosorbents from water. *Environment international*, *123*, 567-579.

Sheng, T., Baig, S. A., Hu, Y., Xue, X., &Xu, X. (2014). Development, characterization and evaluation of iron-coated honeycomb briquette cinders for the removal of As (V) from aqueous solutions. *Arabian Journal of Chemistry*, *7*(1), 27-36.

Shrestha, S., Dhami, A. K., &Nyachhyon, A. R. (2021). Adsorptive Removal of Fe (II) By NaOH Treated Rice Husk: Adsorption Equilibrium and Kinetics. *Scientific World*, *14*(14), 75-82.

Shukla, S. K. (2020). Rice husk derived adsorbents for water purification. *Green Materials for Wastewater Treatment*, 131-148.

Soleimani, M., Davodi, B., &Eisazadeh, H. (2011). Removal of arsenic from aqueous solution using polyaniline/rice husk nanocomposite. *Korean Journal of Chemical Engineering*, *28*, 1532–1538.

Tamaki, S., &FrankenbergerJr, W. T. (1992). Environmental biochemistry of arsenic. *Reviews of Environmental Contamination and Toxicology: Continuation of Residue Reviews*, 79-110.

Tan, K. L., & Hameed, B. H. (2017). Insight into the adsorption kinetics models for the removal of contaminants from aqueous solutions. *Journal of the Taiwan Institute of Chemical Engineers*, *74*, 25-48.

Tian, Y., Wu, M., Lin, X., Huang, P., & Huang, Y. (2011). Synthesis of magnetic wheat straw for arsenic adsorption. *Journal of hazardous materials*, *193*, 10-16.

Timalsina, H., Mainali, B., Angove, M. J., Komai, T., & Paudel, S. R. (2021). Potential modification of groundwater arsenic removal filter commonly used in Nepal: A review. *Groundwater for Sustainable Development*, *12*, 100549.

Ural, N. (2021). The significance of scanning electron microscopy (SEM) analysis on the microstructure of improved clay: An overview. *Open Geosciences*, *13*(1), 197-218.

Vahidnia, A., Van der Voet, G. B., & De Wolff, F. A. (2007). Arsenic neurotoxicity—a review. *Human & experimental toxicology*, *26*(10), 823-832.

Velazquez-Jimenez, L. H., Arcibar-Orozco, J. A., & Rangel-Mendez, J. R. (2018). Overview of As (V) adsorption on Zr-functionalized activated carbon for aqueous streams remediation. *Journal of Environmental Management*, *212*, 121–130.

W., S., Sadegh-Zadeh, F., &Jalili, B. (2014). Characterization of biochars produced from oil palm and rice husks and their adsorption capacities for heavy metals. *International Journal of Environmental Science and Technology*, *11*.

Wang, J., &Guo, X. (2020). Adsorption kinetic models: Physical meanings, applications, and solving methods. *Journal of Hazardous materials*, *390*, 122156.

Yadav, V., Tiwari, D. P., & Bhagat, M. (2019). Arsenic removal using chemically modified Kigelia Africana as a low-cost bio-adsorbent: Equilibrium, Kinetics and Thermodynamics studies. *Int. J. Basic Appl. Res*, *9*, 1282-1294.

Zhang, L., Zhu, T., Liu, X., & Zhang, W. (2016). Simultaneous oxidation and adsorption of As (III) from water by cerium modified chitosan ultrafine nanobiosorbent. *Journal of hazardous materials*, *308*, 1-10.

Zou, Y., Zhang, R., Wang, L., Xue, K., & Chen, J. (2020). Strong adsorption of phosphate from aqueous solution by zirconium-loaded Ca-montmorillonite. *Applied Clay Science*, *192*, 105638.

APPENDIX

Table A_1: Absorbance value of arsenomolybdenum blue complex formed from 0.5 mg/L of As(III) at different wavelength.

Wavelength (nm)	Absorbance
790	0.252
800	0.256
810	0.262
820	0.266
830	0.271
840	0.277
850	0.272
860	0.268
870	0.265
880	0.259
890	0.255

Table A_2: Absorbance value of arsenomolybdenum blue complex at different concentration of As(III) measured at wavelength of 840 nm.

Concentration (mg/L)	Absorbance
0	0
0.01	0.004
0.05	0.011
0.1	0.018
0.2	0.046
0.3	0.075
0.4	0.099
0.5	0.131
0.6	0.157
0.7	0.174
0.8	0.209
0.9	0.227
1	0.259

Table A_3: Effect of pH on adsorption of As(III) on RH

Initial pH	Final pH	Initial concentration (mg/L)	Final concentration (mg/L)	% Absorbance
2.02	2.15	2	1.993	0.35
3.09	3.21	2	1.982	0.9
4.11	4.91	2	1.947	2.65
5.05	6.87	2	1.905	4.75
6.04	7.33	2	1.851	7.45
7.03	7.66	2	1.803	9.85
8.01	7.96	2	1.779	11.05
9.08	8.94	2	1.712	14.4
10.02	10.03	2	1.822	8.9
11.09	10.54	2	1.878	6.1
12.07	11.39	2	1.911	4.45

Table A_4: Effect of pH on adsorption of As(III) on Zr(IV)-RH

Initial pH	Final pH	Initial concentration (mg/L)	Final concentration (mg/L)	% Absorbance
2.03	2.27	2	1.419	29.05
3.01	3.21	2	1.309	34.55
4.04	5.08	2	1.117	44.15
5.03	6.91	2	0.902	54.9
6.05	7.22	2	0.829	58.55
7.06	7.59	2	0.693	65.35
8.01	7.91	2	0.564	71.8
9.08	9.01	2	0.309	84.55
10.34	10.01	2	0.378	81.1
11.23	10.96	2	0.606	69.7
12.01	11.78	2	0.871	56.45

Table A_5: Effect of contact time on adsorption of As(III) onto Zr(IV)-RH

Time (min)	**Initial concentration (mg/L)**	**Equilibrium concentration (mg/L)**	**q_t (mg/g)**	**q_e-q_t (mg/g)**	**log(q_e-q_t)**	**t/q*Table 1:***
1	2	1.777	0.178	1.332	0.124	5.605
5	2	1.562	0.350	1.16	0.064	14.269
10	2	1.291	0.567	0.9432	-0.025	17.630
15	2	1.157	0.674	0.836	-0.077	22.241
30	2	1.011	0.791	0.7192	-0.143	37.917
45	2	0.917	0.866	0.644	-0.191	51.939
60	2	0.814	0.948	0.5616	-0.250	63.237
90	2	0.558	1.153	0.3568	-0.447	78.016
120	2	0.387	1.290	0.22	-0.657	92.994
180	2	0.219	1.424	0.0856	-1.067	126.333
300	2	0.115	1.465	0.0448	-1.348	204.694
1440	2	0.119	1.510	0	0	953.389

Table A_6: Effect of concentration of sample solution on the adsorption of As(III) onto Zr(IV)-RH

Conc. (mg/L)	**C_i (mg/L)**	**C_e (mg/L)**	**q_e (mg/L)**	**C_e/q_e (/L)**	**logC_e**	**logq_e**
0.5	0.46	0.021	0.3512	0.059	-1.677	-0.454
1	0.89	0.15	0.592	0.253	-0.823	-0.227
2	1.99	0.31	1.344	0.230	-0.508	0.128
5	5.06	2.38	2.144	1.110	0.376	0.331
10	9.55	5.64	3.128	1.803	0.751	0.495
25	26.09	13.61	9.984	1.363	1.133	0.999
50	55.07	37.09	14.384	2.578	1.569	1.157
100	108.47	79.19	23.424	3.380	1.898	1.369
150	153.98	111.91	33.656	3.325	2.048	1.527
200	211.65	166.72	35.944	4.638	2.221	1.555
300	315.78	269.01	37.416	7.189	2.429	1.573
400	409.11	361.07	38.432	9.395	2.557	1.584

Table A_7: R_L value for all initial concentration of As(III)

C_i(mg/L)	$R_L = \frac{1}{1 + K_L . C_i}$
0.46	0.99
0.89	0.98
1.99	0.96
5.06	0.9
9.55	0.83
23.21	0.68
45.01	0.52
81.72	0.37
130.08	0.27
177.14	0.22
260.25	0.16

Table A_8: Effect of interfering anions on the adsorptive removal of As(III) onto Zr(IV)-RH

Initial concentration of As(III)= 1.22 ppm

Conc. of added anions (mg/L)	**After Nitrate addition**		**After Silicate addition**		**After Sulphate addition**		**After Phosphate addition**	
	Conc. (mg/L)	**% removal**	**Conc. (mg/L)**	**% removal**	**Conc. (mg/L)**	**% removal**	**Conc. (mg/L)**	**% removal**
0	0.16	86.88	0.16	86.88	0.16	86.88	0.16	86.88
10	0.21	82.78	0.23	81.14	0.25	79.50	0.28	77.04
50	0.25	79.50	0.27	77.86	0.29	76.22	0.31	74.59
100	0.27	77.86	0.29	76.22	0.31	74.59	0.33	72.95
200	0.29	76.22	0.32	73.77	0.35	71.31	0.36	70.49

Table A_9: Desorption of As(III) using NaOH of different molar concentrations

Molar Conc. Of NaOH solution	**Conc. of As(III) in equilibrated filtrate (mg/L)**	**q (desorption) (mg/g)**	**% (Desorption)**
0.05	9.18	3.06	15.11
0.1	33.07	11.02	54.43
0.5	39.51	13.17	65.03
1	51.14	17.04	84.18
2	56.02	18.67	92.21